WARTIME REPORT

ORIGINALLY ISSUED
February 1945 as
Advance Restricted Report 4F28

HEAT-TRANSFER COEFFICIENTS FOR AIR FLOWING IN ROUND TUBES, IN RECTANGULAR DUCTS, AND AROUND FINNED CYLINDERS

By Roger E. Drexel and William H. McAdams
Massachusetts Institute of Technology

NACA

WASHINGTON

NACA ARR No. 4F28

NATIONAL ADVISORY COMMITTEE FOR AERONAUTICS

ADVANCE RESTRICTED REPORT

HEAT-TRANSFER COEFFICIENTS FOR AIR FLOWING IN ROUND TUBES, IN RECTANGULAR DUCTS, AND AROUND FINNED CYLINDERS

By Roger E. Drexel and William H. McAdams

SUMMARY

This report reviews published data and presents some new data.

The available data for heat transfer to air in straight ducts of rectangular and circular cross section have been correlated in plots of Stanton number versus Reynolds number to provide a background for the study of the data for finned cylinders. Equations are recommended for both the streamline and turbulent regions, and data are presented for the transition region between turbulent and laminar flow. Use of hexagonal ends on round tubes causes the characteristics of laminar flow to extend to high Reynolds numbers.

Average coefficients for the entire finned cylinder have been calculated from the average temperature at the base of the fins and an equation which was derived to allow for the effectiveness of the fins.

Heat-transfer coefficients for similar typical fins are in good agreement even though different test techniques and methods of heating were used. The surface coefficient of heat transfer is a complex function of a number of variables, such as width, spacing, and shape of the fins; the mass velocity of the air; the nature of the surface; and the design of the baffles. The test data cover, although incompletely, the ranges of turbulent and laminar flow, and the intermediate transition region. The effects of varying the spacing and width of the fins are irregular. Because of these complications it is impossible to correlate all these results by an

equation and it is believed that further data are needed. The available results for each finned cylinder are correlated herein in terms of graphs of Stanton number versus Reynolds number. In general, for a given Reynolds number, the Stanton number increases with increases in both spacing and width of the fins, and is apparently independent of cylinder diameter and temperature difference.

For a given coefficient of heat transfer improved baffles and rough or wavy surfaces give a substantial reduction in pumping power per unit of heat transfer surface and a somewhat smaller decrease in pressure drop.

INTRODUCTION

The rational design of air-cooled finned cylinders requires the computation of heat transfer and pressure drop, as related to various design variables and operating conditions. Pressure drop is treated in numerous references; for example, pressure drop for sea-level conditions and a variety of finned cylinder designs are given in reference 1, and the effect of altitude is treated in references 2 and 3 and in a report by F. H. Erdman, W. M. S. Richards, K. Campbell, and R. W. Young, Wright Aeronautical Corporation, July 1943. Consequently pressure drop will not be treated in the present study except in connection with certain new data discussed herein. Design conditions, which may affect the coefficient of heat transfer from the metal surfaces to the air stream, include factors such as cylinder diameter, width and spacing of the fins, roughness of the surface, and the type and extent of the baffles or jackets. The surface heat-transfer coefficient from metal to air may also depend on operating conditions, such as mass velocity and temperature difference. Extensive data as to the effect of certain of these factors had been obtained by various workers but were reported in a number of different ways, making it difficult to compare the various sets of published results.

The objects of this investigation are to collect the existing data for heat-transfer coefficients for blower-cooled finned cylinders, to select a suitable common basis of comparison, to ascertain any discrepancies which exist, and to determine the effects of the several factors on the heat-transfer coefficients. This study excludes tests made with cylinders exposed to a free stream with unknown velocity through the passages between the fins.

Since the air passages on a finned cylinder are curved ducts, data for straight ducts of rectangular and circular cross section are correlated for comparison with those for the finned cylinders. The data for straight passages are also of interest in the design of certain types of aircraft heat exchangers.

The cooperation of Pratt and Whitney Aircraft, Harrison Radiator Division of General Motors, and General Electric, in making available heretofore unpublished data, is appreciated.

This investigation, conducted at the Massachusetts Institute of Technology, was sponsored by and conducted with the financial assistance of the National Advisory Committee for Aeronautics.

SYMBOLS

A area of heat transfer surface, square inches

a $(2h/kt)^{0.5}$, inches

C correction factor in equation for effectiveness, dimensionless:

C_C for curvature

C_T for taper

c_p specific heat at constant pressure, Btu/pound $^{\circ}F$

D diameter, inches:

D_b, diameter at base of fins

D_e, equivalent diameter = 4 (cross section)/(perimeter)

D_h, diameter of helix

d prefix indicating differential quantity

E pumping power per unit surface based on over-all pressure drop, foot-pounds per hour per square foot

e height of elementary protuberance characterizing roughness or waviness of surface, inches

G mass velocity, pounds/hour square inch of total cross section

G_{max} mass velocity, pounds/hour square inch of minimum cross section

g acceleration due to gravity, inches/hour^2

h surface coefficient of heat transfer, Btu/hour square inch $^{\circ}F$

h_a, based on arithmetic mean ΔT

h_i, based on initial ΔT

h_L, based on logarithmic mean ΔT

h_x, based on local ΔT

h', as defined in reference 37

j heat-transfer factor, $(h/cG)(c\mu/k)^{2/3}$, dimensionless

j_L heat-transfer factor, $(h_L/cG)(c\mu/k)^{2/3}$, dimensionless

K dimensional constant, defined by the relation

$$U/cG = K\Delta T^{-1/8}$$

k thermal conductivity, Btu/hr square inch $^{\circ}F$ per inch

L nominal length of gas travel, inches

q rate of heat transfer, Btu/hour

R radius, inches:
R_b, at base of fins

r ratio of cross section of duct to that of air passages around cylinder, dimensionless:

r_f, based on duct section at front of model

r_r, based on duct section at rear of model

S cross section of air passages around cylinder, square inches

s mean spacing between fins, inches:

s_b, at base of fins

t mean thickness of fin, inches:

t_t at tip of fin

T air stagnation temperature, °F

T_1 at inlet

T_2 at outlet

T_{sm} mean surface temperature of fin, °F

T_{wm} mean wall temperature at base of fin, °F

U apparent coefficient of heat transfer based on mean difference in temperature between fin base and air, and area of fin base, Btu/hour square inch °F

W mass rate of flow of air, pounds per hour

w width (radial length) of fin, inches:

$w' = w + (t_t/2)$

X product of dimensionless ratios used in converting between h_a, h_i, and h_L:

$X_a = (h_a/cG)(A/S)$

$X_i = (h_i/cG)(A/S)$

$X_L = (h_L/cG)(A/S)$

Y correction factor to allow for effect of curvature of coil on h, dimensionless:

$Y = 1 + (3.5\ D_e/D_H)$

Dimensionless Groups (Consistent Units)

A/S Ratio of heat transfer surface to cross section of air passage

DG/μ Reynolds number

h/cG Stanton number:

$$\frac{h}{cG} = \frac{S}{A} \frac{(T_2-T_1)}{\Delta T}$$

hD/k Nusselt number

$\frac{D_e^3 \rho_f^2 g \beta \Delta T}{\mu^2_f}$ Grashof number

Greek

α portion of half cylinder covered by baffle or jacket, degrees:

α_f, degrees covered on front quarter

α_r, degrees covered on rear quarter

β volumetric coefficient of expansion of gas, taken as reciprocal of temperature in $^{\circ}F$ absolute, for perfect gases

Δp over-all drop in pressure, expressed in inches or centimeters of water, as specified

ΔT difference in temperature between metal and gas, $^{\circ}F$:

ΔT_a, based on arithmetic mean

$\Delta T_a'$, based on equation (8)

ΔT_i, based on initial air and mean surface

ΔT_L, based on logarithmic mean

ΔT_m, mean temperature difference in general

ΔT_o, based on outlet air and mean surface

ΔT_r, based on air and surface at exit

η effectiveness of fin, dimensionless

μ viscosity, pounds/hour inch; divided values from graph of μ versus T by 12

ρ density of air, pounds/inches^3

ρ_{av}, based on $(T_1 + T_2)/2$

ρ_{sc}, based on standard conditions (70° F and normal barometer)

Φ product of terms defined in equation (5)

Note: In many of references cited, the coefficients of heat transfer were given in the rather unusual units of British thermal units per hour per square inch per degree Fahrenheit. The retention of these units for the coefficients, and the desire to keep symbols the same as in the broad field of heat transfer, forced the specification of rather unusual units for several quantities. The units given in the foregoing will produce the correct values of the several dimensionless ratios, but if desired the latter may be evaluated by employing consistently the technical system of units, based on pounds force, pounds matter, feet, hours, degrees Fahrenheit and British thermal units.

HEAT TRANSFER IN STRAIGHT DUCTS

Analysis

At present heat-transfer correlations are based on theoretical analyses, analogies between friction and heat transfer, and empirical equations based on test data. Regardless of the basis, the pertinent equations or curves are generally expressed in terms of dimensionless groups, usually Nusselt number (hD_e/k) and Reynolds number (D_eG/μ). There are a number of reasons for correlating the Stanton number (h/c_pG) instead of hD_e/k, in terms of D_eG/μ (reference 4).

1. The stanton number is numerically equal to an apparatus constant (S/A) times the temperature rise of the fluid divided by the temperature difference:

$$\frac{h}{c_p G} = \frac{GSc_p (T_2 - T_1)}{cG\ A\ \Delta T_m} = \frac{S}{A} \frac{T_2 - T_1}{\Delta T_m} \qquad (1)$$

and consequently the calculation of $h/c_p G$ does not involve specific heat or mass velocity.

2. The only property of the fluid which must be known to calculate both terms in this type of correlation is the viscosity for which accurate values are available.

3. This method of correlation accentuates any changes in the heat-transfer coefficient due to change in type of fluid flow.

4. In the turbulent range, as the Reynolds number is varied, the Stanton number changes less than the Nusselt number.

Throughout this report Stanton numbers are used instead of Nusselt numbers.

It is well known, reference 5, that other dimensionless groups can affect the correlation. The groups $c_p\mu/k$ and either μ_s/μ or μ_f/μ are used to allow for variation in the properties of the fluid; geometrical ratios L/D_e and e/D_e introduce the dimensions of the apparatus and roughness of the test surface; the Grashof number allows for effects of natural convection. In general, a correlation involving a number of fluids and surfaces and a wide range of operating variables must include many of these groups. If the correlation is to be restricted to a single gas such as air, the Prandtl number $c_p\mu/k$ and the viscosity ratio μ_s/μ may be omitted for practical purposes.

This complex situation for flow in round tubes is treated in detail in reference 4. For substantially incompressible turbulent flow of air in round tubes, the data of many workers lead to the dimensionless correlation (reference 5):

$$\frac{h}{c_p G} = 0.028 \left(\frac{DG}{\mu}\right)^{-0.2} \qquad (2)$$

which is also used (reference 5) for flat ducts by substituting D_e for D. The effect of highly compressible flow, of importance at high altitudes, is treated in reference 6.

Assuming undistorted parabolic distribution of velocity for streamline flow, with heat transfer only by radial conduction, mathematical analysis for constant wall temperature (reference 7) shows that $(h_L/c_pG)(L/D_e)$ is a series function of the group cGD_e^2/kL $[= (D_e G/\mu)(c_p\mu/k)(D_e/L)]$ as shown in figure 1.

The function for air in round tubes can be approximated by the following pair of equations (reference 7):

In the streamline region (with D_eG/μ between 2300 and 16.2 L/D_e)

$$\frac{h_L}{c_p G} = 1.98 \left(\frac{L}{D_e}\right)^{-1/3} \left(\frac{D_e G}{\mu}\right)^{-2/3} \qquad (3)$$

and in the streamline region for smaller values of D_eG/μ,

$$\frac{h_L}{cG} = 4.92 \left(\frac{D_e G}{\mu}\right)^{-1} \qquad (3a)$$

For air flowing in flat ducts of high aspect ratio (width/spacing), reference 7 gives the following equations:

With D_eG/μ between 2300 and 94.7 L/D_e

$$\frac{h_L}{c_p G} = 2.26 \left(\frac{L}{D_e}\right)^{-1/3} \left(\frac{D_e G}{\mu}\right)^{-2/3} \qquad (4)$$

and in the streamline region for smaller values of D_eG/μ

$$\frac{h_L}{c_p G} = 10.4 \left(\frac{D_e G}{\mu}\right)^{-1} \qquad (4a)$$

The results of these experimentally verified equations for constant wall temperature, are summarized in figure 2A for round tubes and in figure 2B for rectangular passages, for length-diameter ratios of 10 and 100. The curve AB is based on equation (2), curve DE is based on equation (3) or (4), and curve EF is based on equation (3a) or (4a). The zone BD represents a transition zone between the turbulent region AB and the streamline region DEF, and because of uncertainty as to the exact width of this zone, the curve is dotted. This region is treated in detail in references 4 and 8. Reference 9, based on data for liquids, suggests that the Stanton number be considered independent of the Reynolds number in the region BC. (Point E is the intersection of equations (3a) and (3) or (4a) and (4); point D is at the beginning of the transition region; point C is at the beginning of the region where the Stanton number is considered independent of the Reynolds number; point B signifies the start of the turbulent region.) Increase in L/D_e lowers h_L/c_pG in the streamline region DF but does not affect the location of the curve AB in the turbulent region. Hence, the dip becomes deeper as L/D_e is increased.

From figures 2A and 2B, for a given large L/D_e, it is seen that the dip is deeper for the round tube than for the rectangular section.

The theoretical equations (3) and (4) do not allow for the effect of natural convection and radial gradients in viscosity. Based on a limited amount of data, reference 4 suggests that these effects could be estimated by multiplying h from the theoretical equations by the term:

$$\phi = \left(\frac{\mu}{\mu_f}\right)^{1/3} \left[1 + 0.015 \left(\frac{D_e^3 \rho_f^2 g \beta \Delta T}{\mu_f^2}\right)^{1/3}\right] \quad (5)$$

In the turbulent region AB the local coefficient of heat transfer is believed to be uniform throughout the length of the tube, except possibly for tubes with small values of L/D_e, and in the EF-section of the streamline region the local coefficient is substantially independent of length according to equations (3a) and (4a). With constant surface temperature T_s and constant local coefficient h_x, the logarithmic mean temperature difference is obtained from the

relation $Wc_p dT = h_x dA\ (T_s - T)$. For the sake of uniformity, this type of temperature difference was used throughout the entire range of Reynolds numbers, in analyzing data for tests involving constant wall temperature.

Physical Properties of Air

The physical properties of air recommended by various sources (5, 10, 11) are presented in figure 3. The values of reference 10 were adopted and are represented by the solid curves. For convenience the Prandtl number for air has been considered constant at 0.74.

Data for Round Tubes

An analysis of all the published data for air in round tubes has been made. The better data (12, 13, 14, 15, 16, 17) are plotted as h_L/c_pG versus DG/μ in figure 4. For Reynolds numbers greater than 10,000 the results for air are correlated by the equation:

$$\frac{h_L}{c_pG} = 0.026 \left(\frac{DG}{\mu}\right)^{-0.2} \qquad (6)$$

Based on data for various fluids, reference 4 finds that the two-thirds power of the Prandtl number is involved. Since $c_p\mu/k$ is 0.74 for air, the corresponding equation is

$$j = \frac{h_L}{c_pG}\left(\frac{c_p\mu}{k}\right)^{2/3} = 0.021 \left(\frac{DG}{\mu}\right)^{-0.2} \qquad (6a)$$

It is noted that the recommended value of the constant (0.026) in equation (6) is 7 percent lower than that given in equation (2) from reference 5. At Reynolds numbers larger than 10,000 the maximum deviation in h_L/c_pG is ±25 percent for the data selected; the deviation would have been substantially increased by including data obtained by less desirable techniques.

At Reynolds numbers smaller than 10,000 the experimental points scatter more widely than at Reynolds numbers larger

than 10,000. It may be seen that the runs of Nusselt made at high pressure give higher coefficients than those at atmospheric pressure, owing to the effect of natural convection, involving high Grashof numbers, $(D^3\rho_f^2 g\beta\Delta T/\mu_f^2)$. This effect of natural convection is apt to be less important in aircraft exchangers because of the use of low pressures and small tube diameters. A second cause of scattering of points in figure 4, at Reynolds numbers below 10,000, is the transition from turbulent to laminar flow which gives a dip in the curve of Stanton number versus Reynolds number, as shown in figure 2A. This effect is illustrated by the data of Nusselt at 1 atmosphere and by the data of Josse at 0.1 atmosphere. Data are inadequate for the transition region for air in round tubes.

Since tubes of small diameter are usually used on aircraft oil coolers, and the equivalent diameters of finned passages are small, a request was made in 1943 for data on round tubes of smaller diameter than those plotted in figure 4. A series of tests was reported by J. W. Godfrey and L. P. Saunders in an unpublished report of The Harrison Radiator Division, General Motors Corporation, on oil-cooler tubes having hexagonal ends. Air was drawn through the steam-heated tubes, and the heat balances always agreed within three percent. The results of these tests and those of reference 18 on hexagonal-end tubes are plotted as h_L/c_pG versus DG/μ in figure 5. For Reynolds numbers greater than 10,000 the data agree well with equation (6) predicted from figure 4. For Reynolds numbers below 2,000 the data for L/D_e of 59.8 agree satisfactorily with the curve predicted by using figure 1 and equation (5). The data for smaller values of L/D_e are higher, as expected. For Reynolds numbers ranging from 2,000 to 10,000, appreciable dips are obtained. The data of reference 19 for round tubes without hexagonal ends do not show a deep dip but agree with the data for hex-end tubes in the turbulent and streamline regions. These results for round-end tubes are verified by preliminary runs on multitubular units, made in this laboratory.

The data of figure 5 indicate that the hexagonal ends cause the effects of laminar flow to extend to higher Reynolds numbers than with round-end tubes. At DG/μ of 7,000 it is seen that the value of h_L/c_pG for L/D of 59.8 is considerably more than for L/D of 43.0. If this trend holds for tubes of the same diameter but different lengths, the average coefficient for the entire length would

be greater for the longer tube than for the shorter one, and hence, the local coefficient must increase with length at this Reynolds number. This effect can be explained if the hexagonal ends are considered to be nozzles which tend to set up a uniform velocity distribution and low initial turbulence. As the fluid flows through the tube, the initial characteristics imposed on the stream by the nozzle are changed to those representative of turbulent flow and the coefficient increases. A hexagonal end is probably an imperfect nozzle, but the available data support the foregoing analysis. This effect is discussed in reference 20.

The difference between the data for round tubes and hex-end round tubes in the transition region may become less evident and even disappear if the air entering the exchanger has turbulent characteristics imposed upon it by bends of other upstream disturbances.

Rectangular Ducts

The available data (7, 21) for rectangular ducts are plotted in figure 6 as j_L versus $D_e G/\mu$. Complete results for the tests of Younts, mentioned in reference 7, have been obtained from R. H. Norris of the General Electric Co. At Reynolds numbers greater than 10,000 the data of Younts and of reference 7 are well correlated by equation (6a) for round tubes if D is replaced by D_c:

$$\frac{h_L}{cG}\left(\frac{c\mu}{k}\right)^{2/3} = 0.021\left(\frac{D_c G}{\mu}\right)^{-0.2} \qquad (6b)$$

or for air

$$\frac{h_L}{cG} = 0.026\left(\frac{D_c G}{\mu}\right)^{-0.2} \qquad (6c)$$

In the streamline range the data of these references are higher than the theoretical predictions of equations (4) and (4a). The results of reference 21 for ducts of large L/D_c are far below the predicted curves. This is probably caused by the method of measuring the exit temperature; thermocouples were placed at the center of the duct exit and would consequently give readings lower than the true temperature of the stream if mixed. This would cause the

reported value of j_L to be low. Failure to provide sufficient mixing becomes more important as the exit air approaches the wall temperature; that is, for low flow rates or ducts of large L/D_e. For this reason the results of Younts for ducts of small L/D_e are probably more reliable in the range reported than those of reference 21 for ducts of large L/D_e.

In tests on a duct (reference 22) involving L/D_e of 77.5, and an aspect ratio of 7.7 a special three-pass baffled mixer was used to make certain that the mean temperature of the exit air was measured. The results are summarized and compared with the theoretical equations and with a curve interpolated for L/D_e of 77.5 from the data of reference 21 in figure 7. In the streamline region the data for this duct lie below the theoretical curve for streamline flow in ducts of infinite aspect ratio, and above that interpolated from the results of reference 21. At D_eG/μ of 3000 the data fall 14 percent below the curve recommended for turbulent flow, equation (6b). At present data for rectangular ducts of L/D_e greater than 77.5 are inconclusive.

Résumé for Straight Ducts

In summarizing the results of this study of the heat transfer for flow of air in straight ducts of round and rectangular cross section, it can be stated that for Reynolds numbers, D_eG/μ, exceeding 10,000, the data obtained by the best techniques are correlated within 25 percent for substantially incompressible flow by equation (6c); for flow at high Mach numbers reference 6 is available. For streamline flow of air, at Reynolds numbers below 2300, heat-transfer data for air are scarce (figs. 4, 5, 6, and 7). Where test data are lacking the best procedure is to use figure 1 together with equation (5), or approximate equations (3) and (3a) for round tubes, and equations (4) and (4a) for rectangular sections, together with equation (5). In some cases, because of small values of D and ρ, Φ reduces to substantially 1. In view of the meager data for straight rectangular ducts of large length-diameter ratios, more experimental data are desireable for various aspect ratios.

HEAT TRANSFER IN FINNED PASSAGES

Analysis

Most of the available data for blower cooling of finned cylinders were obtained from tests on electrically heated models, which tend to give approximately constant flux with respect to the air travel around the cylinder, in contrast to the tests of flow in ducts with constant wall temperature. As shown in reference 23, with turbulent flow the local coefficient of heat transfer varies only some ±20 percent as the air flows around a jacketed cylinder. Reference 7 has shown analytically that the minimum local coefficient for laminar flow in straight flat ducts, with constant heat flux, is given by the equation:

$$\frac{h_x}{cG} = 11.2 \left(\frac{D_e G}{\mu}\right)^{-1} \qquad (7)$$

At higher Reynolds numbers, but still with streamline flow, the local coefficient decreases with increase in tube length, but this range is comparatively unimportant, since the coefficient soon approaches the constant value given by equation (7). Hence, as a fair approximation, throughout a large range of Reynolds numbers, the local coefficient of heat transfer may be considered constant. With constant heat flux, if the thermal conduction along the wall is unimportant, both the temperature of air and that of the surface will rise linearly with length, and at the same rate. It is clear that a constant coefficient may be calculated from the temperature difference defined by the equation:

$$\Delta T'_a = T_{sm} - \frac{T_1 + T_2}{2} \qquad (8)$$

The use of this type of an arithmetic temperature difference for data involving electric heating and a logarithmic mean temperature difference for cases involving steam heating of finned cylinders makes the coefficients for the two cases comparable. With moderate mass velocity through the finned passages the temperature of the outlet air can exceed the mean temperature of the fins, thereby giving a negative value to $T_{sm}-T_2$ and precluding the use of a logarithmic mean of $T_{sm}-T_1$, and $T_{sm}-T_2$.

On air-cooled cylinders the average surface temperature, T_{sm}, of the finned surface is of secondary interest. The purpose of cooling and finning is to reduce the temperature at the base of the fins. Consequently nearly all of the references report only the average temperature at the base of the fins, T_{wm}. Since the temperature at the base of the fins is of primary interest, a correlation of surface coefficients should involve the fin base temperature; this temperature and a mathematical effectiveness of the fins are used herein to calculate the average surface coefficient. In design of cylinders, the procedure is reversed and the calculated surface coefficients and the mathematical effectiveness are combined to give the fin base temperature. Furthermore, it is known that surface coefficients, based on the measured mean temperature of the fins, often differ from those based on measured base temperatures and a calculated effectiveness. Consequently both the correlation of test data and the design procedure based thereon should involve base temperatures and calculated effectiveness, so that any errors, due to differences between measured and calculated effectiveness, are not involved.

To obviate a trial-and-error solution in calculating surface coefficients from test data, since the effectiveness is a function of the then unknown surface coefficient, it is customary to calculate an over-all coefficient U, based on the area at the roots of the fins and the over-all temperature difference.

$$\Delta T_a = T_{wm} - \frac{T_1 + T_2}{2} \qquad (9)$$

and to solve graphically for the surface coefficient h by using a curve based on the approximate equation (13) of reference 25:

$$U = \frac{h}{s+t}\left[\frac{2}{a}\left(1 + \frac{w}{2R_b}\right)\tanh aw' + s_b\right] \qquad (10)$$

wherein $a = \sqrt{2h/kt}$ and $w' = w + 0.5\,t_t$.

An alternate equation:

$$U = \frac{h}{s+t}\left[\left(2w' + \frac{ww'}{R_b} + \frac{wt_t}{2R_b}\right)\eta + s_b\right] \qquad (11)$$

is derived in appendix A. It is recommended that η, the effectiveness of the fin, be calculated as the sum of an approximate effectiveness, a correction factor for curvature, C_C, and a correction factor for taper C_T as given by the relation:

$$\eta = \frac{\tanh aw'}{aw'} + C_C + C_T \qquad (12)$$

The factors C_C and C_T may be evaluated from figure 8, taken from reference 26. Equation (11) reduces to equation (10) if the term $wt_b/2R_b$, which is usually negligible, is omitted and if η is taken equal to $(\tanh aw')/aw'$ as would be allowable for a fin of constant cross section. Equation (11) was used in this study in calculating the surface coefficient h from U.

There are only two essential differences between an air-cooled cylinder and a straight rectangular duct. The entrance and exits are different and the flow passages are curved in the former. The effect of curvature for turbulent flow in a round tube is small according to the only available reference (27) which suggests predicting the coefficient for a helically coiled tube by multiplying the heat-transfer coefficient for straight tubes by the term, $Y = 1 + 3.5\ D_e/D_H$. For the maximum value of D_e/D_H usually encountered in finned cylinders (0.067), Y is 1.23. For a normally finned barrel Y would be 1.1, and would be even less for fins of smaller spacing.

Details of Apparatus

Only tests in which the Reynolds number through the finned passages was known and where sufficient data were reported to determine the surface heat-transfer coefficient, h, are considered in this report. The test procedures are described in the original references. Pertinent dimensions of the fins and jackets or baffles are given in table I. The baffle and jacket designs used are shown in figures 9A-9E.

Comparison of Data from Different Sources

A comparison between the data of different sources for similar fins and approximately similar baffles or jackets is shown in figure 10. The data of references 23 and 28 are

for identical fins and the data of references 29 and 31 are for similar fins. The several references did not use identical baffles or jackets, and this probably accounts for some of the differences. Excluding the data of reference 31 and of Pratt and Whitney report 429 by H. B. Nottage and D. S. Hersey, for a given Reynolds number the maximum deviation in Stanton number is only ±10 percent which is less than the deviation of ±25 percent shown in figure 4 for straight round tubes, and is considered good agreement. The data in Pratt and Whitney report 429 are for a finned section the upper part of which was identical with those of references 23 and 28 but the lower part of which had fins tapering to a smaller width. These data lie 30 percent below the curves for references 23, 28, and 29 but further tests with an improved apparatus are showing results higher than those plotted. The data of reference 31 lie 30 percent below those of references 23, 28, and 29, but this may be due to the fact that reference 31 employed highly tapered fins. All the data of figure 10 lie above the theoretically minimum coefficient of heat transfer.

Effects of Fin Spacing and Width

The most extensive tests covering a wide range of both fin spacing, s, and fin width, w, are those of reference 29, the detailed data for which are given in reference 30. As shown by table I, the fin spacing ranged from 0.010 to 0.200 inch, the fin width ranged from 0.37 to 3.00 inches, and the average thickness ranged from 0.026 to 0.050 inch. The ratio r of the cross section at the smallest section of the inlet or outlet portions of the jackets, to the free area through the finned passages, ranged from 0.90 to 2.04. The portion of the cylinder jacketed is specified in terms of angles α_f and α_r for the front and rear halves of the cylinder. These angles are defined in figure 9A and are listed in table I. All the cylinders used by reference 29, except cylinders 39 and 40, the data for which are plotted separately, had a diameter of 4.66 inches at the base or root of the fins, and the results are plotted as Stanton number versus Reynolds number for constant fin width in figures 11A to 11E, with fin spacing specified on the curves.

For a fin width of 0.67 inch, shown in figure 11D, the results show four significant effects:

1. For a given Reynolds number, the Stanton number increases with increase in fin spacing, even though the Reynolds number includes the hydraulic diameter which takes differences

in fin spacing into account. Although increase in the Grashof number, which involves D_e^3, tends to increase the Stanton number, the expected change evaluated from equation (5) is much too small to explain the large increase in h/cG. Unfortunately the coefficients for the finned passages having a small spacing cannot be compared with straight duct data, as no data are available on straight passages with such small equivalent diameter. It may be that the coefficient of heat transfer would be low for straight ducts of small equivalent diameter.

2. Some of the curves are not straight lines, thus suggesting transitions.

3. The dashed line in figure 11D is based on equation (7) for the theoretical minimum local coefficient of heat transfer in straight flat ducts with uniform heat flux. It is seen that the curves for fin spacings ranging from 0.048 to 0.101 inch seem to be asymptotically approaching equation (7) and lie above it, while those for unusual spacings of 0.010 and 0.022 inch lie below it. The broken curve for the upper right portion of figure 11D is the recommended equation for turbulent flow in straight rectangular passages, equation (6c). It is seen that most of the data fall below this line.

4. Since the slopes of the curves are both positive and negative, and often the slope for any one fin width and spacing varies, it seems clear that results for various values of w and s cannot be represented by a single curve in terms of h_a/cG, D_eG/μ, w, and s.

In figure 11 the data for other fin widths show the same characteristics as those for the width of 0.67 inch, although the trends are not always as regular. Since the fin widths of 0.85 and 1.66 inches used with fin spacings of 0.20 inch were not employed with other spacings, the two sets of data are not plotted in figure 11, but do appear in figure 13.

Further data which show the effect of fin spacing upon the Stanton number are presented in reference 32 as plots of Nusselt number based on a logarithmic mean temperature difference versus Reynolds number. The data were reduced to the coefficient h by means of equation (10) in the original reference. Various segments of finned cylinders having different fin spacings but constant widths were tested on an

electrically heated unit. The segment of the cylinder tested was so adjusted that L/s was constant and L/D_e was approximately constant. The results of these tests are plotted on figure 12 as h_I/cG versus D_eG/μ. The data are correlated fairly well by this plot; no large difference between the results of the fin spacings of 0.125 and 0.016 inch are noticed. If plotted as h_a/cG, the data for the different spacings would still be correlated fairly well since h_a/cG is a function of only h_I/cG and S/A (appendix B) both of which are approximately the same, at a fixed Reynolds number, for all the segments tested. Figure 11 indicates that the results are widely different when data are taken for constant L, constant w, and various spacings or values of D_e. Thus the data of figures 11 and 12 seem to indicate that L/D_e is a pertinent variable for tests in this range of D_eG/μ. Attempts to correlate the data of figure 11 in terms of the ratio L/D_e were abandoned since plots showed this parameter would not correlate data having the unusual variations noted.

These same data, of references 29 and 30, are replotted in figures 13A to 13E as h_a/cG versus D_eG/μ for constant fin spacing, with the values of fin width specified on the curves. For a given Reynolds number, the Stanton number h_a/cG usually increases with increase in fin width, but exceptions are noted. This effect seems quite marked for fin spacings ranging from 0.022 to 0.101 inch. This effect had previously been noted in reference 29 for finned cylinders tested in a free stream with unknown velocity through the finned passages but had not been mentioned in connection with blower cooling tests.

Reference 31 tested cylinders provided with fins of various widths and spacings, but used fins of triangular cross section in contrast to the fins of rectangular cross section employed by reference 29. Table I describes the fins and jackets. The data were reported only in the form of plotted points, from which values of h_a/cG and D_eG/μ were calculated and are shown in figure 14. For each spacing (0.236 and 0.118 inch), for a given Reynolds number, h_a/cG decreases with increase in fin width, which is exactly opposite to the results of reference 29 shown in figures 13A to 13E. However, in reference 31 the decrease in fin width was accompanied by a substantial increase in jacket coverage and this effect may offset the effect of changing fin width

shown by the results of reference 29. For a given fin width, comparison of results for triangular fins shown in figure 14 reveals that for a given Reynolds number and average thickness of fin, h_a/cG decreases as fin spacing decreases from 0.236 to 0.118. For these fins all the data lie above equation (7) for the theoretically minimum local coefficient of heat transfer.

In the tests of reference 29 discussed in the foregoing, as shown in table I, the clearance between the tip of the fin and the jacket was 0.01 inch. Reference 33 reports tests for fin spacings of 0.102 and 0.200 inch and fin widths from 0.67 to 1.22 inches, and employed a gap of 0.125 inch between the jacket and the tips of the fins. These results, if plotted, would show the usual effect of fin spacing and a somewhat increased effect of fin width for a spacing of 0.200 inch.

The other available data for finned cylinders (28, 34, 35, Pratt and Whitney report 429 by H. B. Nottage and D. S. Hersey, and Pratt and Whitney report 446 by J. W. Miller, H. B. Nottage, and D. S. Hersey) are plotted in figure 15. Contrary to the effect of spacing shown in figure 11, figure 15A shows substantially no effect of spacing in the range from 0.048 to 0.100 inch. All the data of figures 15B and 15C lie above equation (7) for the theoretically minimum local coefficient of heat transfer and the data of reference 34, plotted in figure 15C, approach equation (7) asymptotically at low Reynolds numbers. However, the data of figure 15A, for small spacings lie below this equation.

Type of Temperature Difference

All of these results were obtained from the average temperature at the base of the fins and the calculated fin effectiveness, as explained earlier in this report. However, the average surface temperatures were reported in reference 30 for the tests of reference 29, which showed that the surface coefficients based on measured surface temperatures usually were somewhat higher than those obtained from base temperatures and calculated effectiveness. The effect of fin width for a given spacing, developed in figure 13, is also found if measured surface temperatures are employed in evaluating the Stanton numbers. The same is true of the effect of fin spacing developed in figure 11.

Throughout this report surface heat-transfer coefficients for runs with electric heat have been based on arithmetic mean temperature difference, as previously explained. In the

past, heat-transfer coefficients have at times (reference 29) been based on the difference between the mean temperature of the surface and the temperature of the inlet air. Figure 16 shows the data of figure 13B replotted in terms of h_i/cG versus D_eG/μ. It is seen that at a given Reynolds number the Stanton number still increases with increase in fin width, an effect not previously noted.

Appendix B gives equations useful for converting reported coefficients from one temperature-difference basis to another.

Effect of Cylinder Diameter

The only source which reports tests for cylinders of different diameters is reference 29. Figure 17 shows data for three similar finned cylinders having base diameters of 3.66, 4.66, and 6.34 inches. At the higher Reynolds numbers the data for the cylinder with D_b equal to 4.66 inches are higher. However, the data for both the smaller and larger cylinders fall below this. On the basis of these results it seems that cylinder diameter has no effect on the Stanton number within the accuracy of the data.

Effect of Surface Conditions

Surface conditions may be classified as rough or wavy or smooth. All the data discussed in the foregoing were obtained with smooth surfaces. Recent reports have contained data for several types of surface. Data from Pratt and Whitney reports 429 and 446 may be combined to show the effect of roughness. Data were obtained for a standard fin and later with a fin of the same nominal dimensions after 1100 hours service and the enamel coating had been chipped; identical baffles were used in both cases. Figure 18 shows that the Stanton number is higher for the rough surface at a given Reynolds number. However, a plot of h/cG versus D_eG/μ is not the most revealing method of comparing different fins as there is no reason that the fin exhibiting the highest Stanton number at a given Reynolds number must also exhibit the highest coefficient for a given pumping power per square foot of heat-transfer surface. A better comparison of the data is presented in figure 19, a plot of $(h/c)(c\mu/k)^{2/3}$ versus $E\rho_{av}^2$, the pumping power expressed as foot-pounds per hour per square foot of heat-transfer surface, times the average fluid density squared. This plot also indicates

that the rough surface is preferred. (Reference 36 shows the utility of this method of comparing flow inside tubes with flow across tube bundles). Since the available pressure drop may be a limitation, figure 20 shows a plot of h_a versus $\Delta p\ \rho_{av}/\rho_{sc}$. The coefficients for the rough surfaces are slightly higher than the smooth surface for the same pressure drop. Thus these data indicate that surface roughening is a method for reducing the pumping power per unit surface by a large percent and slightly increasing the coefficient of heat transfer for a given pressure drop. In using these data it must be remembered that only the nominal thickness of the fins was available and was employed in calculating the fin effectiveness. It is possible that the actual thickness of one or both of the fins was slightly different from the nominal thickness.

Although it is useful to compare heat-transfer coefficients at a given pressure drop or pumping power per unit area, it should be emphasized that conditions giving the highest coefficient may have the lowest air flow rate and consequently the highest average air temperature at a given heat flux. The exact effect of these compensating factors on the wall temperature depends on operating conditions. Allowances must also be made for variations in air temperature when pressure drop or pumping power are compared at a given coefficient.

Reference 37 reported results for smooth and wavy surfaces tested with three different baffles. These were 90 complete waves in the special fins. These waves approximated sine curves and had a peak to valley distance of 0.022 inch at the fin root and 0.033 inch at the fin tip. The cylinders were heated with hot water and the results were extrapolated to infinite water velocity in determining the coefficients of heat transfer. Although the reference states that allowances were made for the cross flow of air and water and for the effectiveness of the fins, it appears that the resistance of the metal (approximately 1/2 inch thick) between the base of the fins and the water was not considered in calculating coefficients. This would cause the reported Stanton numbers to be low; the data as plotted on figure 21 are lower than the other data previously considered. Consequently the coefficient, h', cannot be compared with other data in this report but may be used to determine the effect of waviness. Figures 21 and 23 indicate that wavy fins give increased coefficients at a given Reynolds number or pumping power per unit surface.

When the data are plotted as h' versus $\Delta p\ \rho_{av}/\rho_{sc}$ (fig. 22), it is found that, for a given pressure drop, waviness increases the heat-transfer coefficient by approximately 5 percent for baffles A and C and approximately 20 percent for baffle B. The percent of the cylinder covered by the baffle, figure 9B, increases from baffle A to baffle C and it would naturally be expected that, if waviness increased the heat-transfer coefficient for a given pressure drop, any trends in the increase would be related to the extent of baffling. This is not the case; for baffle B waviness increased the heat-transfer coefficient more than for other baffles. This result is not immediately explainable; it may be that this variation is within the accuracy of the data.

Maximum and Minimum Temperatures

The hottest spot on an air-cooled cylinder usually occurs at the rear of the cylinder and it is therefore desirable to know this temperature as well as the average surface temperature upon which the heat-transfer coefficient is based. A correlation of data based on tests of electrically heated models, where there was no propeller swirl, may not apply directly to engine installations. However, the data from reference 30 and from Pratt and Whitney reports 429 and 446 were plotted as the ratio $\Delta T_r/\Delta T_a$ versus Reynolds number, but no consistent trends with fin spacing and width were found. Ideally, if the coefficient of heat transfer may be obtained from correlations such as figure 11; the average temperature difference can be calculated for any heat flux. Correlations of $\Delta T_r/\Delta T_a$ would permit the temperature differences at the rear of the cylinder and the actual rear temperature to be calculated. This type of correlation should include factors such as baffle shape to allow for differences in flow conditions and cylinder wall thickness to allow for thermal conduction from rear to front.

Another approach to this problem, more fundamental than the empirical one suggested, is to measure actual local coefficients of heat transfer as has been done in reference 23. This type of data will allow accurate prediction of the cylinder temperatures after proper allowances are made for conduction around the cylinder, which obviously will be dependent on the thickness of the cylinder wall and that of the muff.

Effect of Temperature Difference

Except for some of the tests of reference 31, the wall temperatures used by the references were well below those of operating air-cooled engines. It is consequently desirable to know the effect of temperature difference on the heat-transfer coefficient so that the available data may be extrapolated to operating conditions. Extensive tests by H. B. Nottage and D. S. Hersey, Pratt and Whitney report 429, indicated that the heat-transfer coefficient, for a given Reynolds number, was inversely proportional to $\Delta T^{1/8}$. This was at first thought to be caused by heat losses but reference 28 obtained the same effect on an identical muff for runs which had heat balances with 6 percent. The temperature difference was varied by changing the electrical input to the test section. These data, corrected to a Reynolds number of 4730, are plotted on figure 24. Also included are results of tests on the apparatus of references 23 and 24, which involved an identical muff and the baffle shown in figure 9E. The heat balances for those tests also agreed within 6 percent. In this case the temperature difference was varied by heating the inlet air. No noticeable effect of temperature difference is shown in these results.

Data of reference 31 corrected to a Reynolds number of 16,700 are plotted in figure 24 and indicate that U_a/cG increases slightly with increase in ΔT_a. These results cannot be trusted as well as can those of Nottage and Hersey, since complete data are not reported.

The data of these different investigators thus show a different but small effect of ΔT. If the two most reliable sets of data are considered (references 24 and 28) it will be noticed that reference 28 used electric heat and reference 24 used steam heat. This may account for the difference noted.

At first it appears that the variation of the coefficient with ΔT for the electrically heated muff might be explained by conduction around the fins. However, if it is accepted that the local coefficient of heat transfer at a given point is a function of only the Reynolds number (24), thermal conduction should not cause this effect. Consider, for example, runs made at the same Reynolds number and two different heat fluxes, one double the other. If conduction is neglected for the moment, the air temperature rise per unit length and the local temperature differences for the high flux should be twice that of the low flux. The curves

of wall temperature and air temperature could be superimposed by changing the temperature scale for one test. The fin temperatures at any point could also be plotted on this new curve and would be found to coincide. If conduction is then allowed for from this curve, it is clear that conduction will have the same effect on each test and hence the coefficient should not change.

Effect of Baffle Shape

The data of references 23, 24, and 37 afford an insight into the results of changing the baffle shape for a given fin spacing and width. The data of reference 37 are plotted in figures 21, 22, and 23. Figure 25 shows the data of references 23 and 24, which employed steam heat, plotted as h_L/cG versus D_eG/μ for the jacket (shown in fig. 9C), a model of a conventional baffle (fig. 9D), and a special baffle (fig. 9E). Both baffles had spacers to keep the baffles a fixed distance from the fin tips. Tests were also made with the spacers removed on the special baffle. Over the range tested, the baffles listed in order of decreasing coefficient, at a constant Reynolds number, are as follows: jacket, special baffle, conventional baffle, and special baffle with spacer removed. It is noted that the curves have slightly different slopes and that the data for the jacket and the conventional baffle, which extend over a wider Reynolds number range than the other data, indicate that the slopes of the curves may get steeper at lower Reynolds numbers. All the data of figure 25 lie above equation (4a) for the theoretically minimum local coefficient of heat transfer for constant wall temperature. Comparison of the data on the basis of pressure drop, (fig. 26) and pumping power per unit surface, (fig. 27) show that baffles listed in order of decreasing coefficient still are: jacket, special baffle, conventional baffle, and special baffle with spacer removed.

Effect of Swirl

A propeller creates turbulence in the air stream and causes flow across the cylinders. It is well known that the flow conditions, set up by the propeller, cool the front of the cylinders better than the flow resulting from blower cooling (reference 38). In runs described in reference 24, a sheet metal insert was placed in front of the test cylinder

as indicated in figure 9E. The ratio of the condensate on the right-hand to that on the left-hand side was substantially the same as before the insertion of this device, and it was concluded that the air flow still divided fairly equally around the two sides of the cylinder. However, the average coefficient of heat transfer increased slightly as indicated on figures 25, 26, and 27. These results are of qualitative value only as no comparison is available between the turbulence in this test and that in the air stream before an actual cylinder in flight.

CONCLUSIONS

1. For flow of air at Reynolds numbers larger than 10,000 in straight ducts, the selected heat-transfer data given herein are correlated within maximum deviations of 25 percent for round tubes (fig. 4) and 10 percent for rectangular passages (fig. 6) by the dimensionless equation:

$$\frac{h}{cG} = 0.026 \left(\frac{D_e G}{\mu}\right)^{-0.2} \tag{6c}$$

using physical properties of reference 10, shown in figure 3. This relation is easier to use than conventional equations involving the Nusselt number and consequently thermal conductivity.

2. For flow of air at Reynolds number smaller than 10,000 in straight ducts, heat-transfer data are inadequate for round and rectangular shapes, except for round tubes with hexagonal ends, correlated in figure 5. The available data for straight rectangular ducts are summarized in figure 6, with

$$j = \left(\frac{h}{cG}\right)\left(\frac{c\mu}{k}\right)^{2/3}$$

plotted versus Reynolds number based on equivalent diameter, for various ratios of length to equivalent diameter. For straight rectangular shapes with L/D_e less than 80, at low Reynolds numbers, the Stanton numbers for air asymptotically approach the values predicted from the theoretical equation for the minimum coefficient in flat ducts:

$$\frac{h}{cG} = 10.4 \left(\frac{D_e G}{\mu}\right)^{-1} \qquad (4a)$$

3. Data for tests on steam-heated and electrically heated blower-cooled cylinders may best be compared if the heat-transfer coefficients are calculated on the basis of logarithmic and arithmetic temperature differences, respectively. On this basis the data of various references for similar muffs, correlated in figure 10 in terms of Stanton and Reynolds numbers, agree surprisingly well in view of differences in methods of testing and in the design of the jackets or baffles. The coefficients for these 1.1 inch fins, having spacings of 0.11 inch are within ±30 percent of those predicted from equation (6c) for turbulent flow in straight rectangular ducts.

4. The Stanton number usually decreases as Reynolds number increases, but the data for a fin having a spacing of 0.01 inch (fig. 11D) shows the opposite trend. As the best line through the data for fins having spacings between 0.048 and 0.101 inch is concave upward and approaches equation (7) at low Reynolds numbers and equation (6c) at high Reynolds numbers (fig. 11D), a transition between laminar and turbulent flow is indicated.

5. For a given Reynolds number, the Stanton numbers usually increase with increase in fin spacing, both for rectangular and triangular fins. (See figs. 11, 14, and 15.)

6. For a given Reynolds number, the Stanton numbers usually increase with increase in fin width for rectangular fins (figs. 13 and 15B), but decrease with increase in fin width for triangular fins (fig. 14).

7. Cylinder diameter has no effect on the coefficient of heat transfer, on the basis of the available data (fig. 17).

8. Temperature difference has a negligible effect on the surface heat-transfer coefficient, in the range of available data (fig. 24).

9. The few available data indicate that rough or wavy surfaces, compared with smooth surfaces, increase the Stanton number for a given Reynolds number; increase the heat-transfer coefficient for a given pumping power per unit surface; and give a small increase in heat-transfer coefficient for a given pressure drop.

10. For a given coefficient of heat transfer, both the pumping power per unit surface and the pressure drop depend on the design of the baffle or jacket. Figures 26 and 27 show that the baffle of figure 9E is superior to that of figure 9D in both these repsects, but these advantages disappear at low flow rates. The jacket of figure 9C is better than either of these two baffles.

Massachusetts Institute of Technology,
Cambridge, Mass., May 24, 1944.

APPENDIX A

DERIVATION OF EQUATION RELATING U AND h

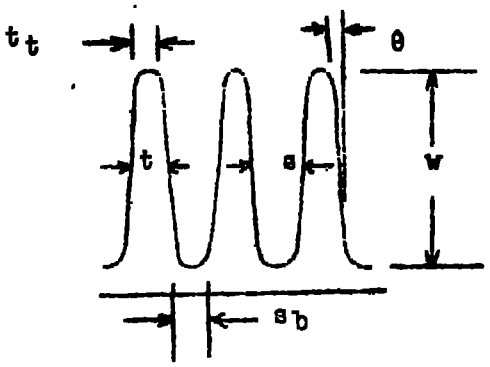

At any given position on a cylinder, if the local surface coefficient is assumed independent of radial position and if cos θ is considered equal to unity:

$$h\left[4\pi\left(R_b+\frac{w}{2}\right)w+2\pi(R_b+w)t_t\right]\eta\Delta T_b+h\,2\pi R_b s_b\Delta T_b$$

$$=U(s+t)2\pi R_b\Delta T_b$$

Letting $w'=w+(t_t/2)$, and rearranging

$$U=\frac{h}{s+t}\left[\left(2w'+\frac{ww'}{R_b}+\frac{wt_t}{2R_b}\right)\eta+s_b\right] \qquad (11)$$

The effectiveness η can be evaluated by the following equation of reference 26.

$$\eta=\frac{\tanh aw'}{aw'}+C_C+C_T$$

with which $a=\sqrt{2h/kt}$ and C_C and C_T are corrections for curvature and taper, respectively, and are evaluated from figure 8.

This equation will reduce to equation (10) if $wt_t/2R_b$ is neglected and if C_C+C_T is assumed equal to zero as for a fin of constant cross section:

$$U=\frac{h}{s+t}\left[\frac{2}{a}\left(1+\frac{w}{2R_b}\right)\tanh aw'+s_b\right] \qquad (10)$$

APPENDIX B

INTERCONVERSION OF STANTON NUMBERS

(For finned surface this method applies to U/$\mathfrak{G}$G only; for nonfinned surface the method applies to h/cG). Combining

$$q = G\, S_c\, (T_2 - T_1)$$

and

$$q = h\, A\, \Delta T$$

gives

$$\left(\frac{h}{cG}\right)\left(\frac{A}{S}\right) = X = \frac{T_2 - T_1}{\Delta T}$$

For constant surface temperature or when the temperature difference is calculated on the basis of a fixed temperature,

$$\left(\frac{h_1}{cG}\right)\left(\frac{A}{S}\right) = X_1 = \frac{\Delta T_1 - \Delta T_2}{\Delta T_1} \qquad (A)$$

$$\left(\frac{h_2}{cG}\right)\left(\frac{A}{S}\right) = X_2 = 2\left(\frac{\Delta T_1 - \Delta T_2}{\Delta T_1 - \Delta T_2}\right) \qquad (B)$$

$$\left(\frac{h_L}{cG}\right)\left(\frac{A}{S}\right) = X_L = \ln \frac{\Delta T_1}{\Delta T_2} \qquad (C)$$

Solving for ΔT_2

$$\Delta T_2 = \Delta T_1\, (1 - X_1) \qquad (A')$$

$$\Delta T_2 = \Delta T_1\, (2 - X_2)/(2 + X_2) \qquad (B')$$

$$\Delta T_2 = \Delta T_1\, e^{-X_L} \qquad (C')$$

By substituting equations (B') and (C') in (A), (A') and (C') in (B), and (A') and (B') in (C), the following table is obtained.

INTERCONVERSION OF STANTON NUMBERS BASED

ON A CONSTANT SURFACE TEMPERATURE

Known

Sought	X_i	X_a	X_L
X_i	—	$\frac{2X_a}{2+X}$	$1-e^{-X_L}$
X_a	$\frac{2X_i}{2+X_i}$	——	$2\left(\frac{1-e^{-X_L}}{1+e^{-X_L}}\right)$
X_L	$\ln\left(\frac{1}{1-X_i}\right)$	$\ln\left(\frac{2+X_a}{2-X_a}\right)$	——

REFERENCES

1. Rollin, V. G., and Ellerbrock, Herman H., Jr.: Pressure Drop Across Finned Cylinders Enclosed in a Jacket. NACA TN No. 621, 1937.

2. Goldstein, Arthur W. and Ellerbrock, Herman H., Jr.: Compressibility and Heating Effects on Pressure Loss and Cooling of a Baffled Cylinder Barrel. NACA ARR No. E4G20, 1944.

3. Becker, John V., and Baals, Donald D.: The Aerodynamic Effects of Heat and Compressibility in the Internal Flow Systems of Aircraft. NACA ACR, Sept. 1942.

4. Colburn, A. P.: A Method of Correlating Forced Convection Heat Transfer Data and a Comparison with Fluid Friction. Trans. Am. Inst. Chem. Eng., vol. 29, 1933, pp. 174-210.

5. McAdams, W. H.: Heat Transmission. McGraw-Hill Book Co., Inc., 1942.

6. McAdams, W. H., Nicolai, L. A., and Keenan, J. H.: Measurements of Recovery Factors and Coefficients of Heat Transfer in a Tube for Subsonic Flow of Air. NACA TN No. 985, 1945.

7. Norris, R. H., and Streid, D. D.: Laminar-Flow Heat Transfer Coefficients for Ducts. Trans. A.S.M.E., vol. 62, 1940, pp. 525-533.

8. Martinelli, R. C., Boelter, L. M. K., Weinberg, E. B., and Yakahi, S.: Heat Transfer to a Fluid Flowing Periodically at Low Frequencies in a Vertical Tube. Trans. A.S.M.E., vol. 65, no. 7, 1943, pp. 789-798.

9. Norris, R. H., and Sims, M. W.: A Simplified Heat-Transfer Correlation for Semi-Turbulent Flow of Liquids in Pipes. Trans. Am. Inst. Chem. Eng., vol. 38, 1942, pp. 469-492.

10. Tribus, Myron, and Boelter, L. M. K.: An Investigation of Aircraft Heaters. II - Properties of Gasses. NACA ARR, Oct. 1942.

11. International Critical Tables: 1, pp. 102-103; 2, p. 312; 5, 2, pp. 80-81, 213-214. McGraw-Hill Book Co., Inc., 1926-1933.

12. Josse, E.: Surface Condensers for Steam Turbines. Engineering, vol. 86, 1908, pp. 802-806.

13. Nusselt, W.: Der Wärmeübergang in Rohrleitungen. Mitteilungen Forschung, vol. 89, 1910, pp. 1-38.

14. Rietschel, H.: (Experiments on Heat Transfer, Lost Pressure Head, and Surface Temperature when Using Large Air Velocities). Mitteilungen Prufungsanstalt f. Heizungs u. Luftungseinrichtungen, Konigl. Techische Hochschule (Berlin 3), Sept. 1910.

15. Guchman, A., Hjunchin, N., Taassowa, W., and Warschawski, G.: Untersuchung des Wärmeüberganges bei Bewegung eines Gasses mit sehr grosser Geschwindigkeit. Tech. Physics of the U.S.S.R., vol. 2, 1935, pp. 375-413.

16. Lelchuk, V. L.: Heat Transfer and Hydraulic Flow Resistance for Streams of High Velocity. NACA TM No. 1054, 1943.

17. Colburn, A. P., and Goghlan, C. A.: Heat Transfer to Hydrogen-Nitrogen Mixtures Inside Tubes. Trans. A.S.M.E., vol. 63, 1941, pp. 561-566.

18. London, A. L., and Brewster, J. I.: Test and Predicted Oil Cooler Performance. Trans. A.S.M.E., vol 66, 1944, pp. 75-80.

19. Graetz, H. G.: Heat Transfer to Air in Tubes. S. B. Thesis in Chem. Eng., M.I.T., Feb. 1944.

20. Bakhmetev, Boris A.: The Mechanics of Turbulent Flow. Princeton Univ. Press, 1941, pp. 51-52.

21. Washington, L., and Marks, W. M.: Heat Transfer and Pressure Drop in Rectangular Air Passages. Ind. Eng. Chem., vol. 29, 1937, pp. 337-345.

22. Hoopes, J. W., Jr., and Rinaldo, P. M.: Heating of Air in Rectangular Ducts. S. B. Thesis in Chem. Eng., M.I.T., Feb. 1944.

23. Goldey, R. H.: Local Heat Transfer Coefficients around a Finned Cylinder. S. M. Thesis in Chem. Eng., M.I.T., Feb. 1944.

24. Drexel, R. E.: Subsequent Tests on the Apparatus of R. H. Goldey. Data on file at the Dept. of Chem. Eng., M.I.T.

25. Biermann, A. E., and Pinkel, B.: Heat Transfer from Finned Metal Cylinders in an Air Stream. NACA Rep. No. 488, 1934.

26. Harper, D. R., III, and Brown, W. B.: Mathematical Equations for Heat Conduction in the Fins of Air-Cooled Engines. NACA Rep. No. 158, 1922.

27. Jeschke, D.: Wärmeübergang und Druckverlust in Rohrschlangen. Z.V.D.I. 69, 1526, 1925; Z.V.D.I. Erganzungsheft 24, 1925.

28. Lemmon, A. W., and Colburn, A. P.: Test of "Conventional" and Diffuser Type Baffles in the University of Delaware Muff Rig. Memorandum Report. Division of Chem. Eng., Univ. of Delaware, April 6, 1944.

29. Ellerbrook, Herman H. Jr., and Biermann, A. E.: Surface Heat-Transfer Coefficients of Finned Cylinders. NACA Rep. No. 676, 1939.

30. Supercharger and Air-Flow Research Division, AERL: Heat-Transfer Data on Blower-Cooled Finned Cylinders. NACA ARR No. E4E12, 1944.

31. Löhner, Kurt: Development of Air-Cooled Engines with Blower Cooling. NACA TM No. 725, 1933.

32. Breevoort, M. J.: Principles Involved in the Cooling of a Finned and Baffled Cylinder. NACA TN No. 655, 1933.

33. Schey, Oscar W., and Ellerbrook, Herman H., Jr.: Blower Cooling of Finned Cylinders. NACA Rep. No. 587, 1937.

34. Foster, H. H., and Ellerbrook, Herman H., Jr.: Cylinder Barrel Cooling with Bonded Preformed Copper Fins. NACA ACR, May 1941.

35. Hartshorn, A. S.: Wind Tunnel Investigation of the Cooling of an Air-Jacketed Engine. R. & M. No. 1641, British A.R.C., 1935.

36. Colburn, A. P.: Heat Transfer by Natural and Forced Convection. Purdue Univ. Eng. Bull. 26, No. 1, 1942, pp. 47-48.

37. Johnson, J. E., and Simpson, E.: Heat Dissipation and Drag Characteristics of Cylinder Barrels with Plain and Waved Fins from Air Duct Experiments. R.A.E. Rep. No. E, 3975, May 1943.

38. Wood, George P., and Breevoort, Maurice J.: Design, Selection, and Installation of Aircraft Heat Exchangers. NACA ARR No. 3G31, 1943.

TABLE I. DETAILS OF FINS AND JACKETS

*Cyl.	Ref.	Note	s	w	t	D_b	α_f	α_r	r_f	r_r
J	23	4,11	0.111	1.11	0.03	6.19	71	71	1.43	1.43
D	24	4,11	0.111	1.11	0.03	6.19	50	62	2.97	2.14
A,B,C,E	24	4,11	0.111	1.11	0.03	6.19	54	66	2.21	1.14
Conv.	28	4,11	0.111	1.11	0.03	6.19	50	66	2.96	1.32
11	29	1,2,5,10	0.131	1.22	0.035	4.66	61	61	1.01	1.01
12	29	1,2,5,10	0.102	1.22	0.035	4.66	61	61	1.08	1.08
13	29	1,2,5,10	0.077	1.22	0.035	4.66	61	61	1.16	1.16
14	29	1,2,5,10	0.048	1.22	0.035	4.66	61	61	1.37	1.37
15	29	1,2,5,10	0.022	1.22	0.035	4.66	61	61	2.04	2.04
18	29	1,2,5,10	0.101	0.97	0.035	4.66	63	63	0.90	0.90
19	29	1,2,5,10	0.077	0.97	0.035	4.66	63	63	0.97	0.97
20	29	1,2,5,10	0.048	0.97	0.035	4.66	63	63	1.14	1.14
21	29	1,2,5,10	0.022	0.97	0.035	4.66	63	63	1.73	1.73
24	29	1,2,5,10	0.101	0.67	0.035	4.66	64	64	0.98	0.98
25	29	1,2,5,10	0.077	0.67	0.035	4.66	64	64	1.05	1.05
26	29	1,2,5,10	0.048	0.67	0.035	4.66	64	64	1.26	1.26
27	29	1,2,5,10	0.022	0.67	0.035	4.66	64	64	1.83	1.83
31	29	1,2,5,10	0.101	0.37	0.035	4.66	65	65	0.98	0.98
32	29	1,2,5,10	0.077	0.37	0.035	4.66	65	65	1.06	1.06
33	29	1,2,5,10	0.048	0.37	0.035	4.66	65	65	1.21	1.21
34	29	1,2,5,10	0.022	0.37	0.035	4.66	65	65	1.83	1.83
35	29	1,2,6,10	0.080	3.00	0.035	4.66	56	56	1.09	1.09
36	29	1,2,6,10	0.055	3.00	0.035	4.66	56	56	1.24	1.24
37	29	1,2,6,10	0.028	3.00	0.035	4.66	56	56	1.70	1.70
38	29	1,2,5,10	0.035	0.37	0.035	4.66	65	65	1.44	1.44
39	29	1,2,5,10	0.124	0.50	0.026	3.66	56	56	1.48	1.48
40	29	1,2,5,10	0.120	0.52	0.030	6.34	66	66	1.33	1.33
57	29	1,2,5,10	0.010	0.67	0.035	4.66	67	67	1.32	1.32
58	29	1,2,5,10	0.200	0.85	0.050	4.66	57	57	1.45	1.45
59	29	1,2,4,10	0.200	1.66	0.050	4.66	51	51	1.45	1.45
C42	31	7,12	0.118	1.654	0.039	6.30	60	60	1.33	1.33
C28	31	7,12	0.118	1.101	0.039	6.30	66	66	1.33	1.33
C14	31	7,12	0.118	0.552	0.039	6.30	75	75	1.33	1.33
C7	31	7,12	0.118	0.275	0.039	6.30	81	81	1.33	1.33
B42	31	7,12	0.118	1.654	0.079	6.30	60	60	1.67	1.67
B28	31	7,12	0.118	1.101	0.079	6.30	66	66	1.67	1.67
B14	31	7,12	0.118	0.552	0.079	6.30	75	75	1.67	1.67
B7	31	7,12	0.118	0.275	0.079	6.30	81	81	1.67	1.67
A42	31	7,12	0.236	1.654	0.079	6.30	60	60	1.33	1.33
A28	31	7,12	0.236	1.101	0.079	6.30	66	66	1.33	1.33
A14	31	7,12	0.236	0.552	0.079	6 30	75	75	1.33	1.33
A7	31	7,12	0.236	0.275	0.079	6.30	81	81	1.33	1.33
1	P&W Rep. 429	7,11	0.111	1.11	0.030	6.19	47	72	2.49	1.37
2		7,11	0.111	1.11	0.030	6.19	47	72	2.49	1.37
3		7,11	0.111	1.11	0.030	6.19	47	72	2.49	1.37
4	P&W Rep. 446	7	0.0578	1.05	0.0255	6.26	47	72	3.02	1.66
5		7	0.048	1.21	0.030	6.2	47	72	2.65	1.46
6		7	0.100	1.10	0.040	6.2	47	72	2.79	1.52
7		5	0.116	0.605	0.025	6.00	47	72	4.27	2.36
8		7,11,1	0.111	1.11	0.030	6.19	47	72	2.49	1.37
9		7	0.110	1.126	0.030	6.16	47	72	2.42	1.34
	32	8,10	0.125	1.00	0.033	5.81		180°	Segment	
	32	8,10	0.0625	1.00	0.025	5.81		90°	"	
	32	8,10	0.031	1.00	0.016	5.81		45°	"	
	32	8,10	0.016	1.00	0.006	5.81		22.5°	"	
	34	6,10	0.123	1.92	0.026	6.13	55	47		
	35	13	0.185	1.00	0.065	6.00			0.987	0.987
Plain Wavy	37	9,11	0.10 0.098	1.235 1.045	0.06 0.062	6.78 7.16			Note 3	

* The cylinder numbers are those used in the original references. 1- Chipped surface. 2- The clearance between the jacket and the fin tips is given in reference 30 as approximately .01". 3- See figure 9b for 3 baffles used. 4- Aluminum alloy. 5- Steel. 6- Copper. 7- Aluminum. 8- Brass. 9- High-silicon aluminum alloy. 10- $t_t/t = 1$ (no taper). 11- $t_t/t = .67$. 12- $t_t/t = 0$ (triangular fin). 13- $t_t/t = .62$. The values of the thermal conductivity of metals presented in reference 5 were used except for the aluminum alloy of note 4. The thermal conductivity of this alloy was given as 8.10 in Pratt and Whitney report 446.

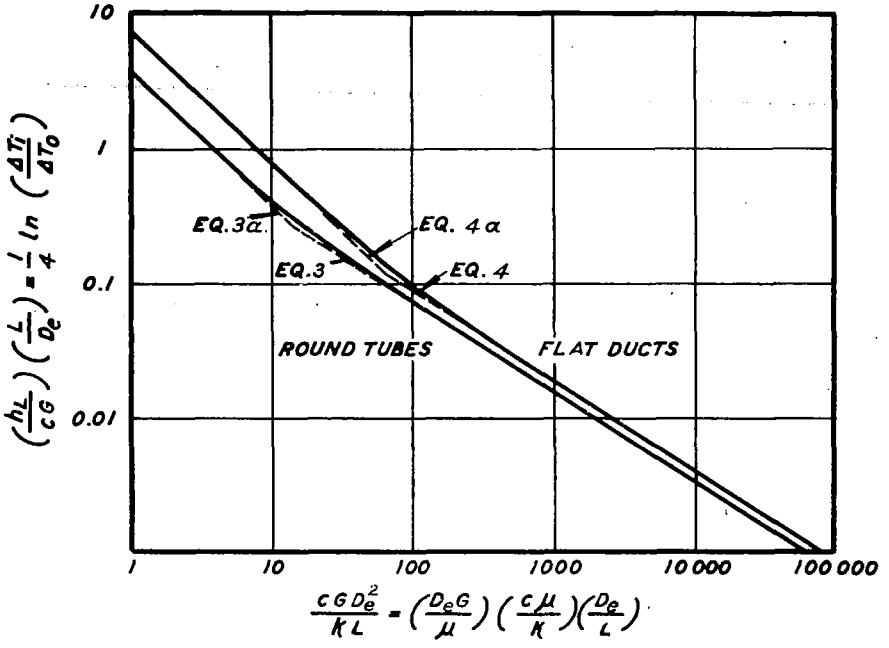

FIGURE 1
PREDICTED RELATIONS FOR LAMINAR FLOW IN DUCTS HAVING CONSTANT WALL TEMPERATURE, NEGLECTING EFFECTS OF NATURAL CONVECTION REF. 7

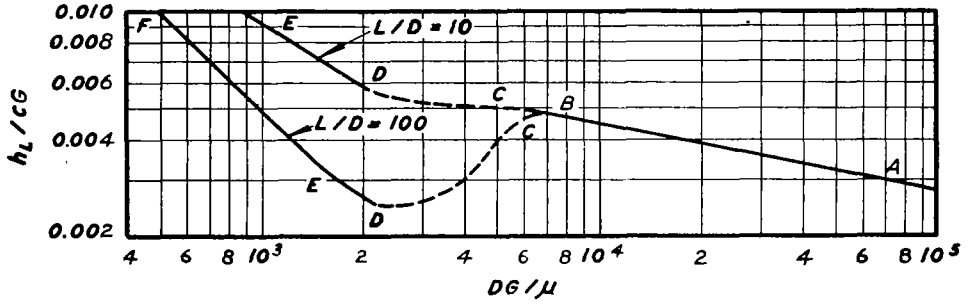

FIGURE 2A
STANTON NUMBER VS REYNOLDS NUMBER FOR AIR FLOWING IN ROUND TUBES HAVING CONSTANT WALL TEMPERATURE

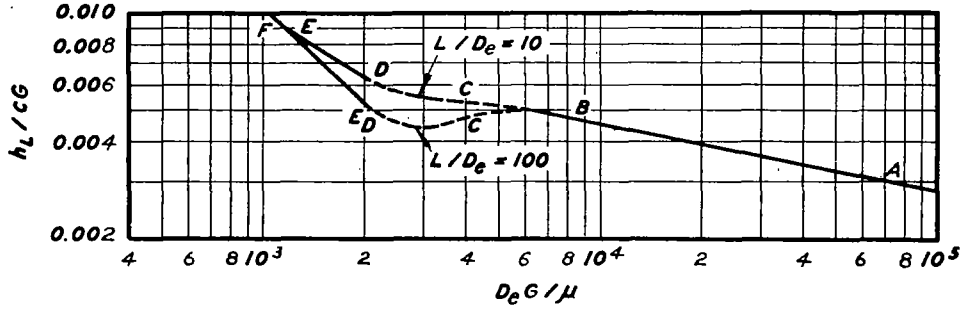

FIGURE 2B
STANTON NUMBER VS REYNOLDS NUMBER FOR AIR FLOWING IN FLAT DUCTS HAVING CONSTANT WALL TEMPERATURE

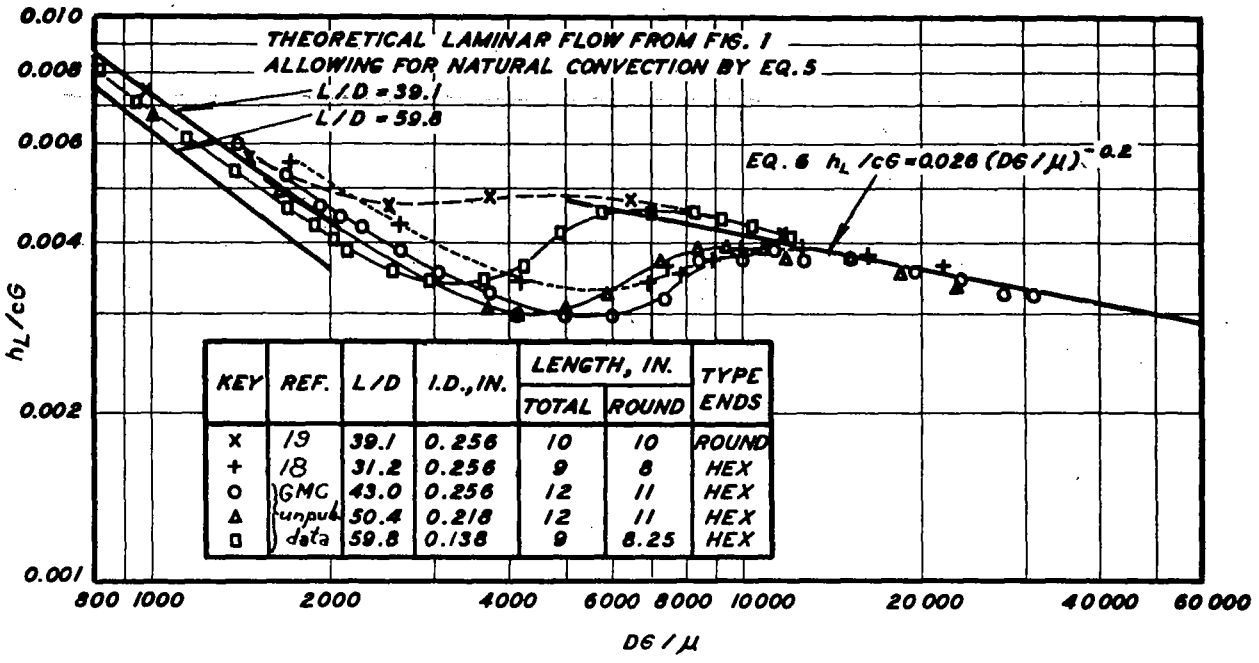

KEY	REF.	L/D	I.D., IN.	LENGTH, IN. TOTAL	LENGTH, IN. ROUND	TYPE ENDS
x	19	39.1	0.256	10	10	ROUND
+	18	31.2	0.256	9	8	HEX
o	GMC unpub. data	43.0	0.256	12	11	HEX
Δ		50.4	0.218	12	11	HEX
□		59.8	0.138	9	8.25	HEX

FIGURE 5
STANTON NUMBER VS REYNOLDS NUMBER
FOR STEAM HEATED STRAIGHT ROUND TUBES
HAVING HEXAGONAL AND ROUND ENDS

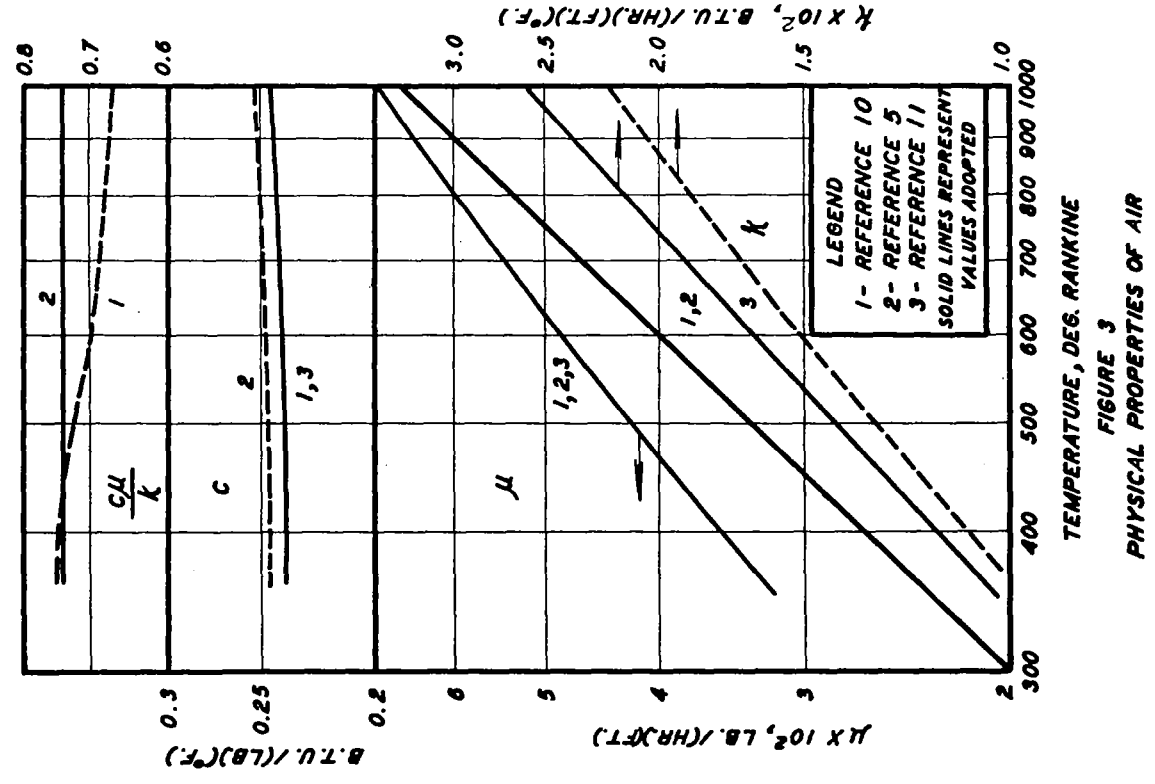

FIGURE 3
PHYSICAL PROPERTIES OF AIR

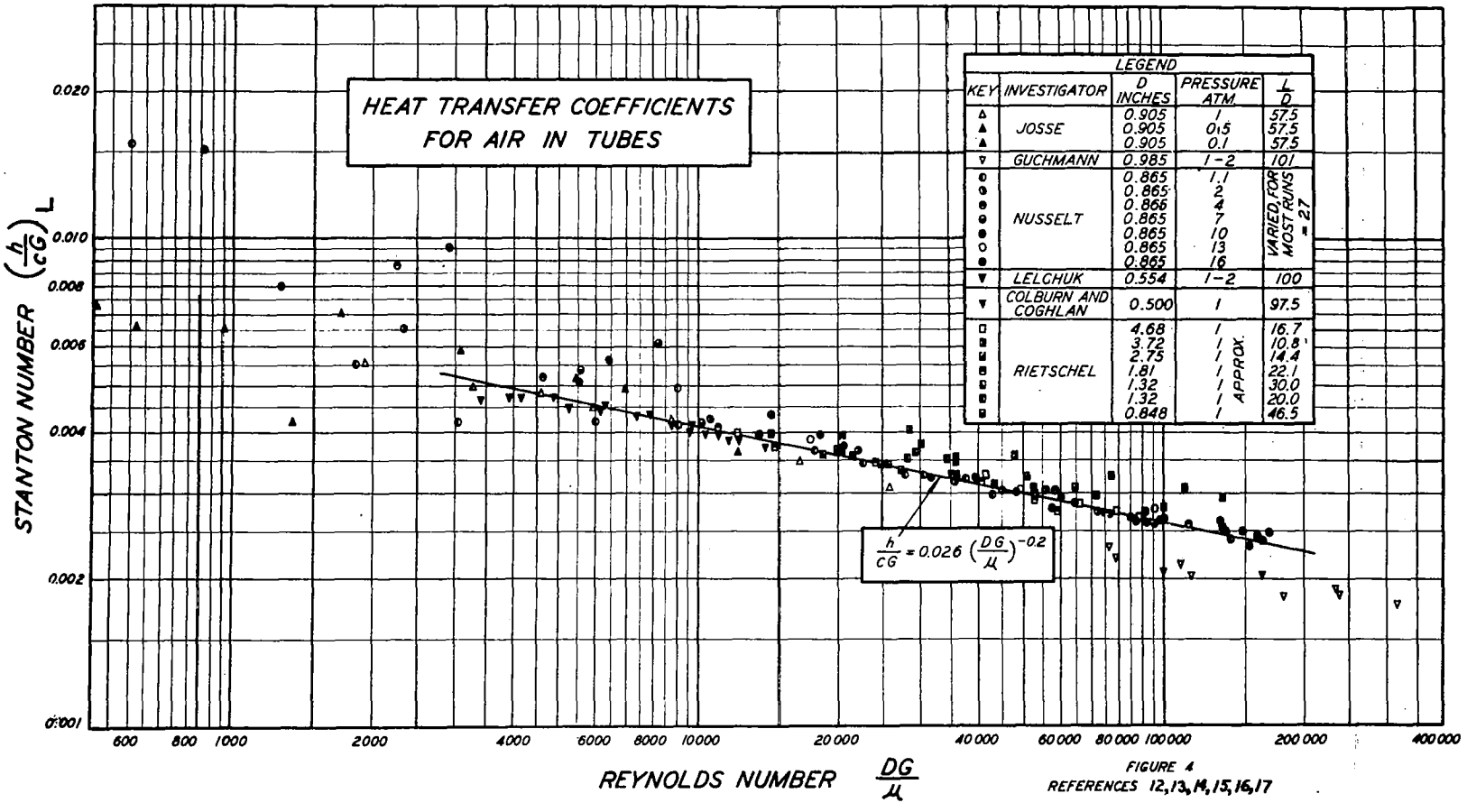

FIGURE 4
REFERENCES 12, 13, 14, 15, 16, 17

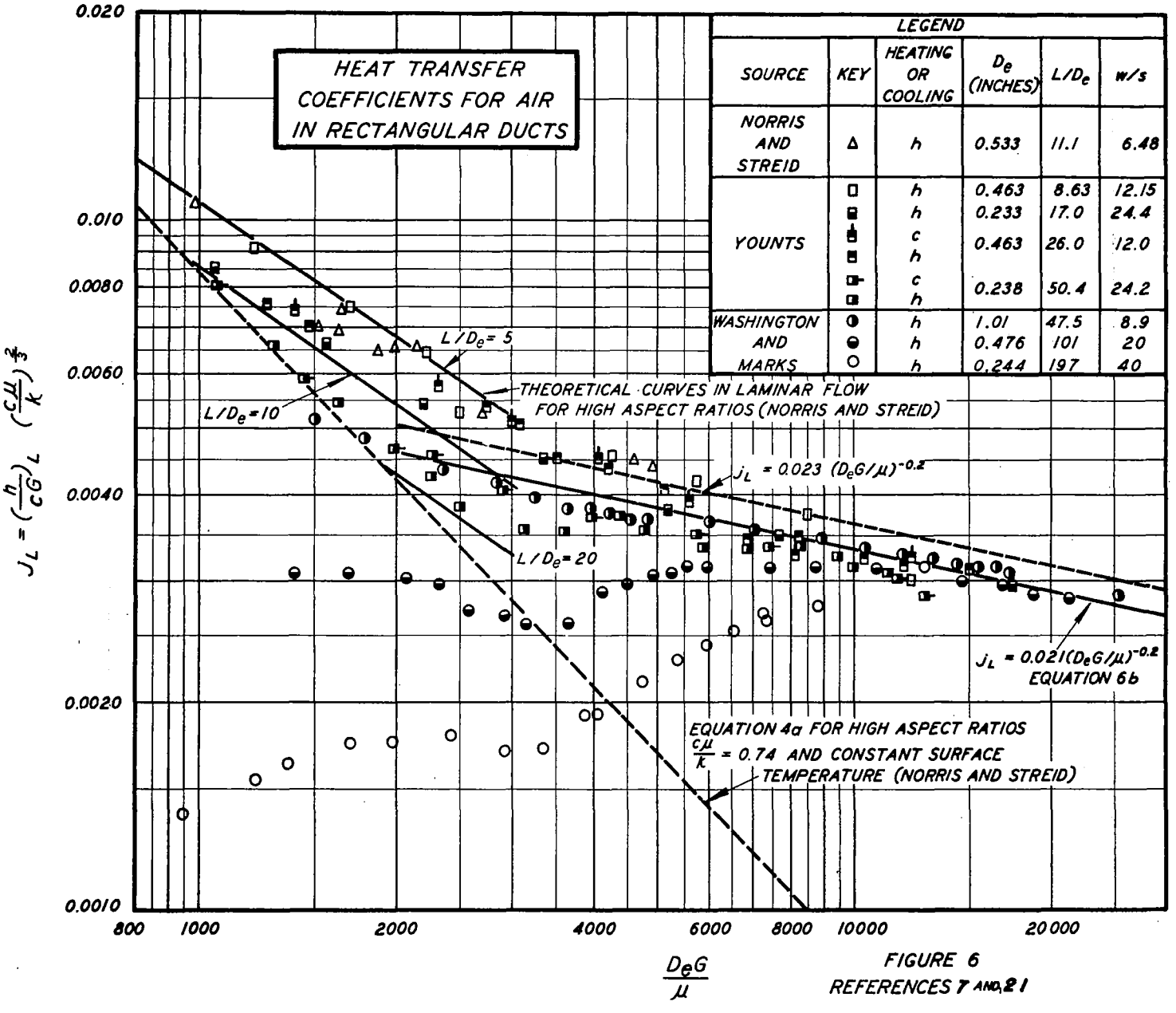

FIGURE 6
REFERENCES 7 AND 21

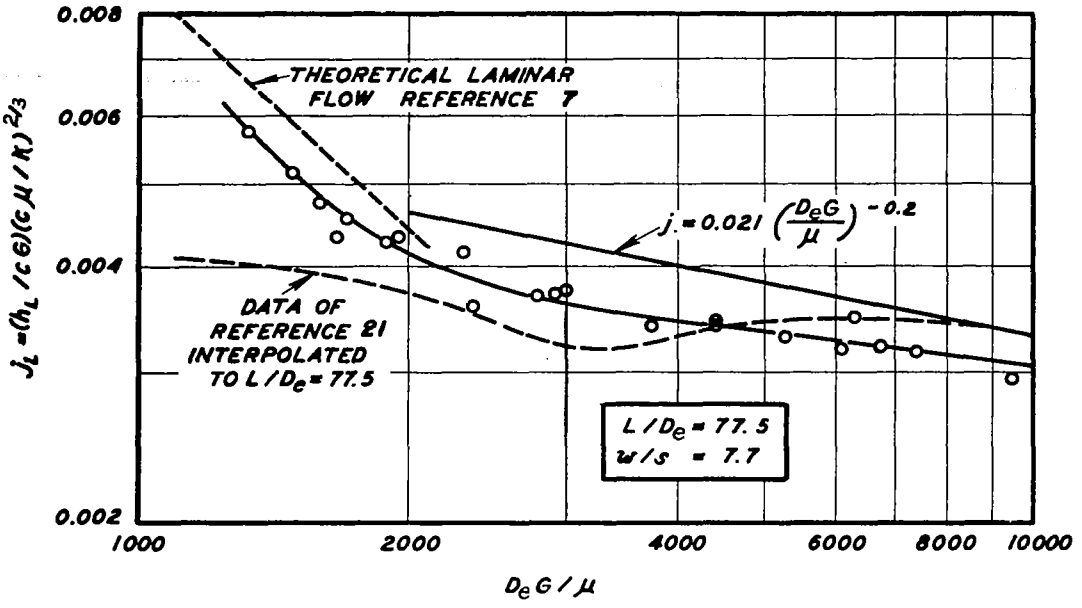

FIGURE 7
HEAT TRANSFER COEFFICIENTS
FOR RECTANGULAR DUCTS
j_L VS $D_e G/U$, DATA OF REFERENCE 22

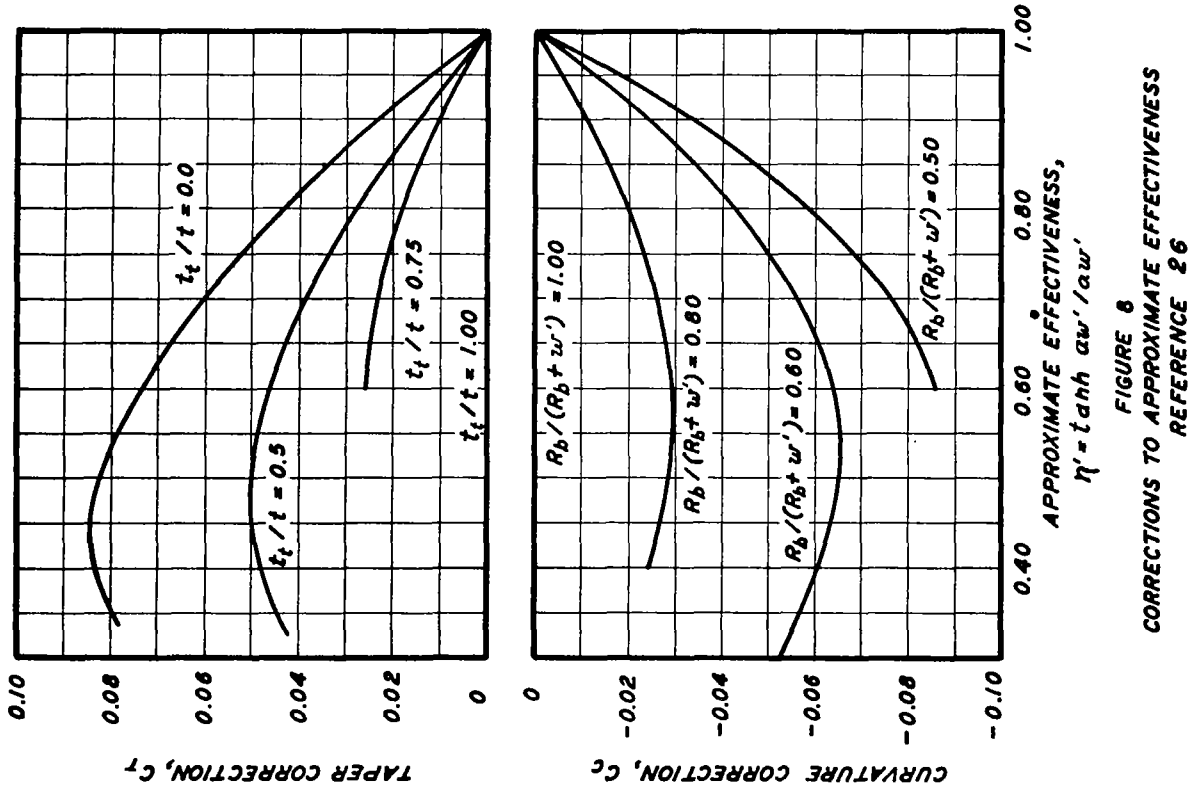

FIGURE 8
CORRECTIONS TO APPROXIMATE EFFECTIVENESS
REFERENCE 26

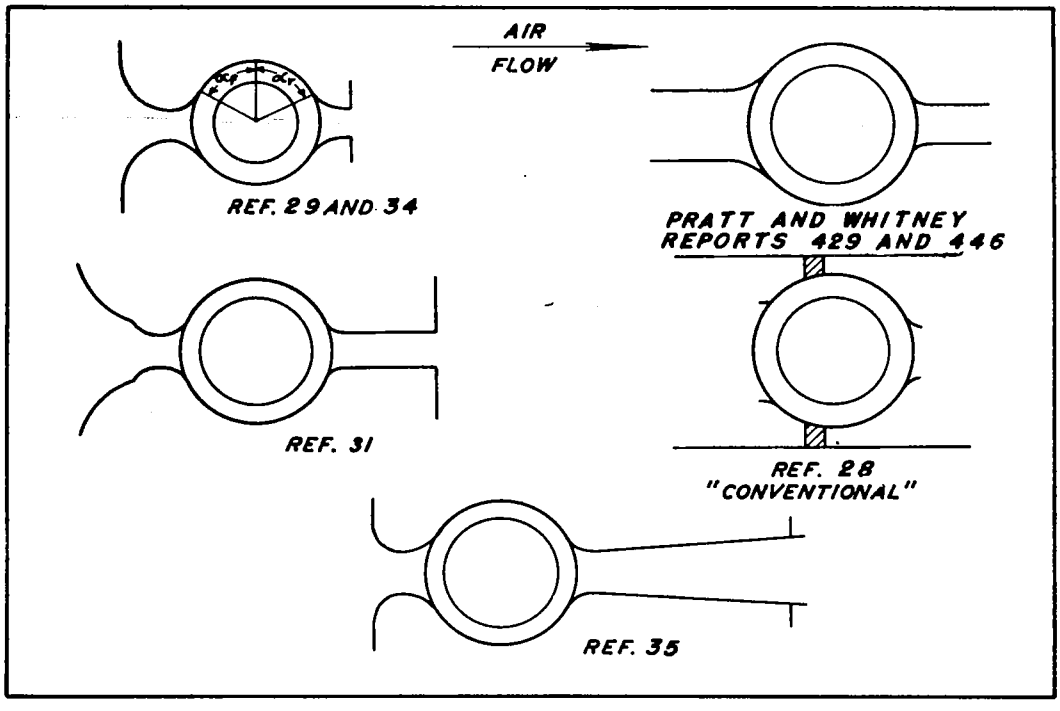

FIGURE 9A
BAFFLE AND JACKET DESIGNS

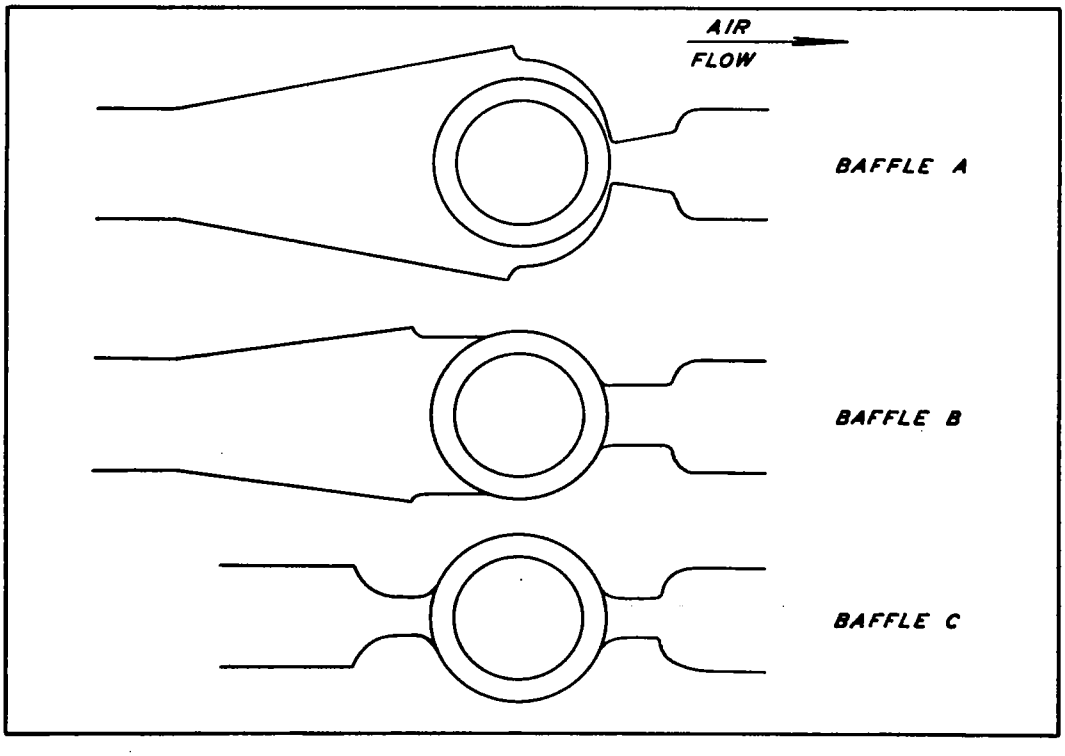

FIGURE 9B
BAFFLE AND JACKET DESIGNS
REFERENCE 37

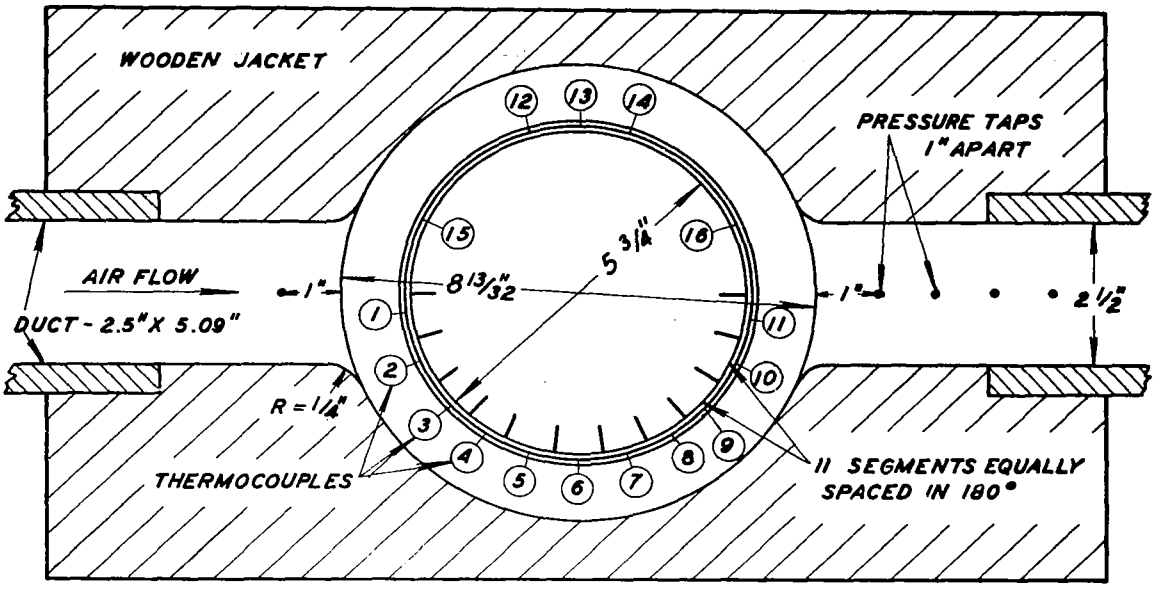

TOP VIEW OF TEST SECTION

SHOWING LOCATION OF PRESSURE TAPS AND THERMOCOUPLES

ALL COUPLES 2" FROM BOTTOM EXCEPT (12) - 1/2", (14) - 1"

FIGURE 9C

REFERENCE 23

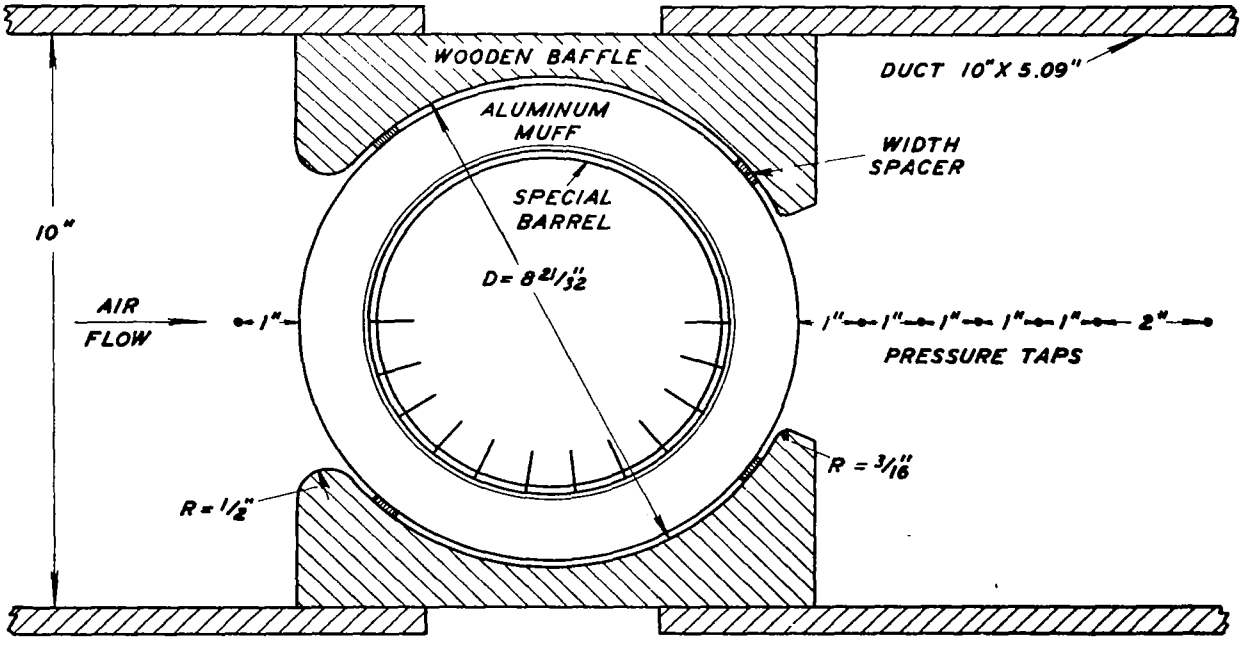

TOP VIEW OF MODEL PRATT AND WHITNEY R2800 ENGINE BAFFLES AS TESTED

(THERMOCOUPLES LOCATED AS SHOWN FOR JACKETED MUFF)

FIGURE 9D

REFERENCE 24

SCALE: 1" = 2"

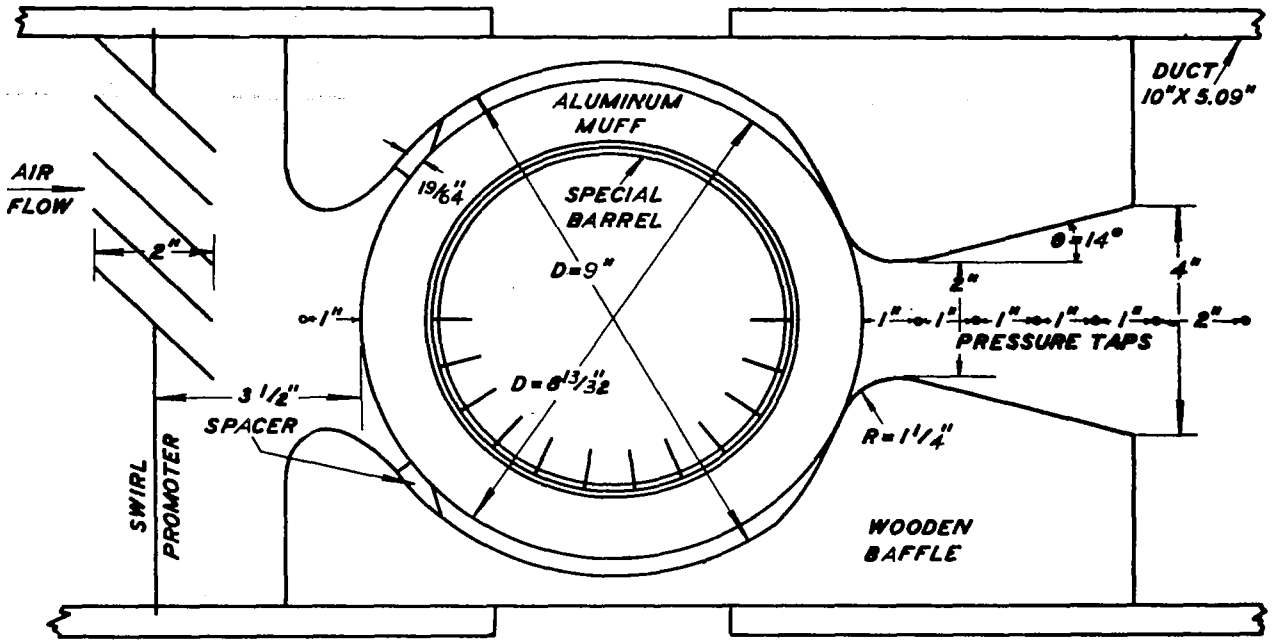

FIGURE 9E
TOP VIEW OF SPECIAL BAFFLE
AND SWIRL PROMOTER
(THERMOCOUPLES LOCATED AS SHOWN FOR JACKETED MUFF)
REFERENCE 24 SCALE: 1"= 2"

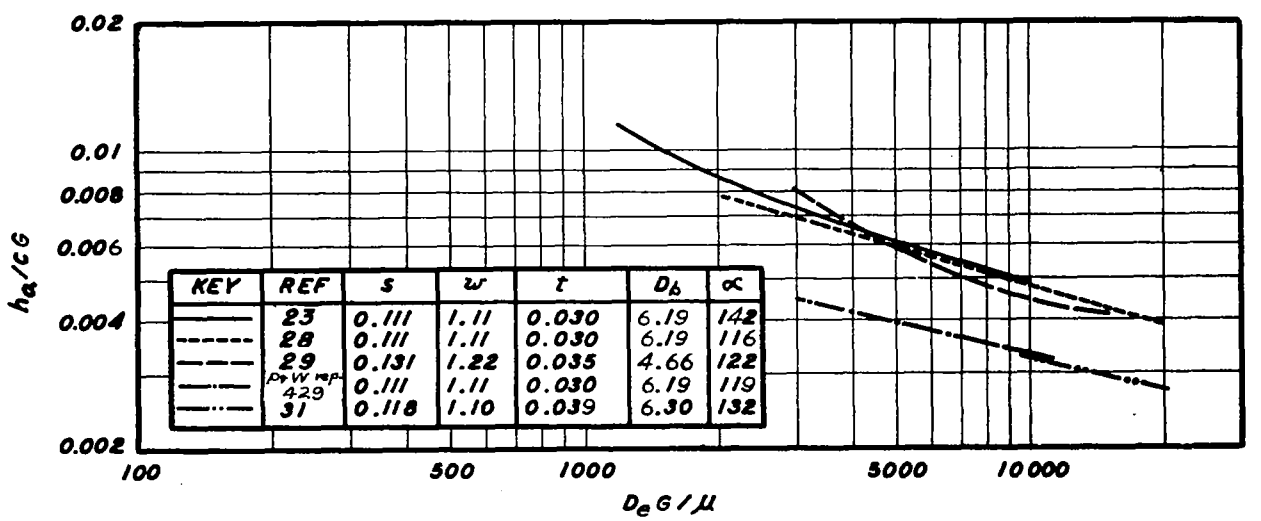

FIGURE 10
COMPARISON OF DATA FROM DIFFERENT
SOURCES HAVING SIMILAR FINS
AND JACKETS

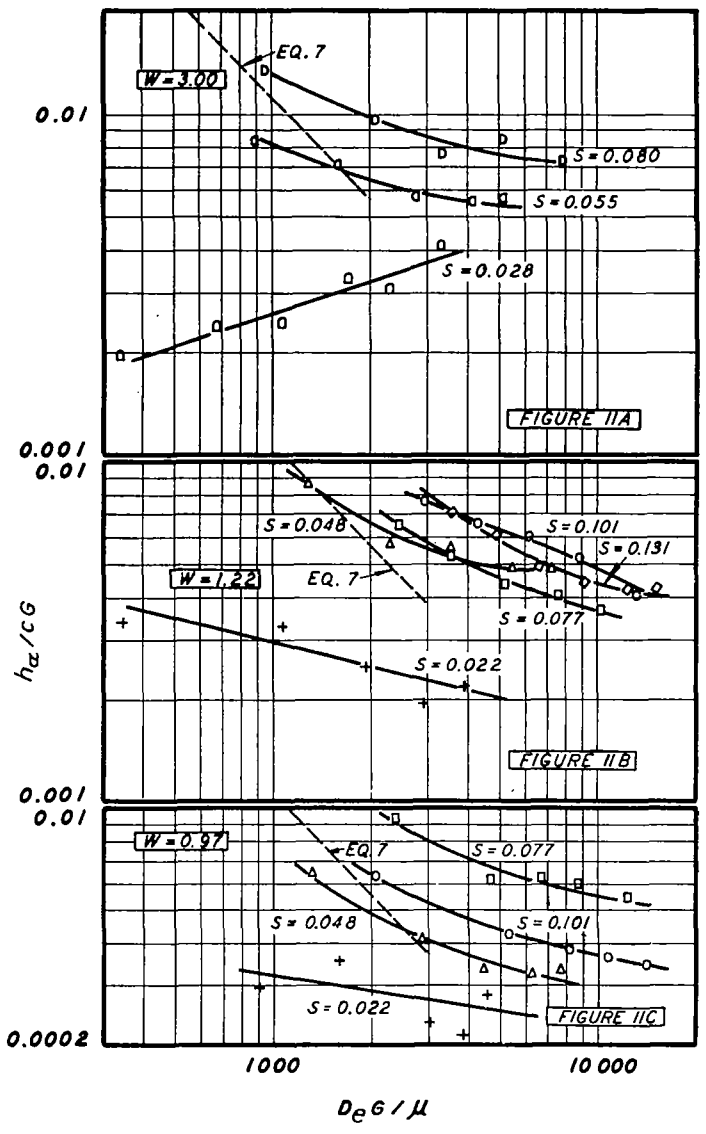

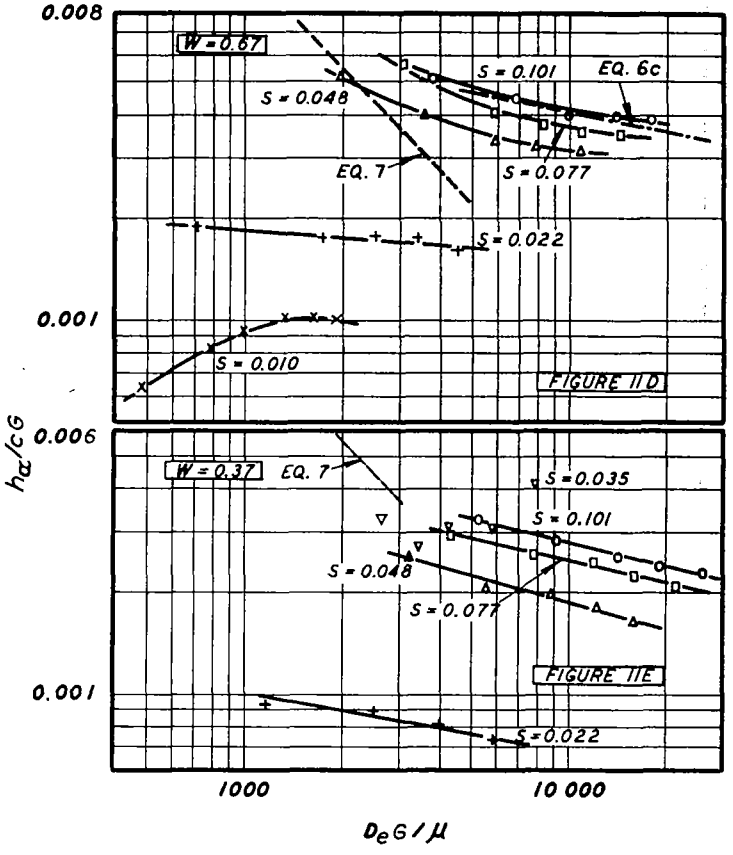

KEY	S	KEY	S
◇	0.131	△	0.048
○	0.101	▽	0.035
▷	0.080	□	0.028
□	0.077	+	0.022
◁	0.055	×	0.010
$D_b = 4.66$		$t = 0.035$	

FIGURE 11
STANTON NUMBER VS REYNOLDS NUMBER FOR FINNED CYLINDERS SHOWING THE EFFECT OF FIN SPACING
REFERENCE 29

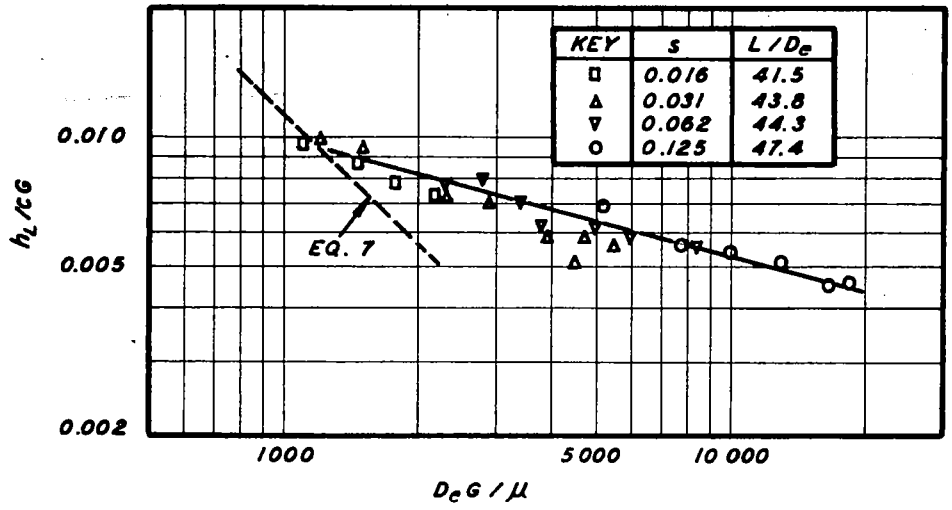

FIGURE 12
STANTON NUMBER VS REYNOLDS NUMBER
FOR SEGMENTS OF FINNED CYLINDERS
WITH APPROXIMATELY CONSTANT L/D_e
REFERENCE 32

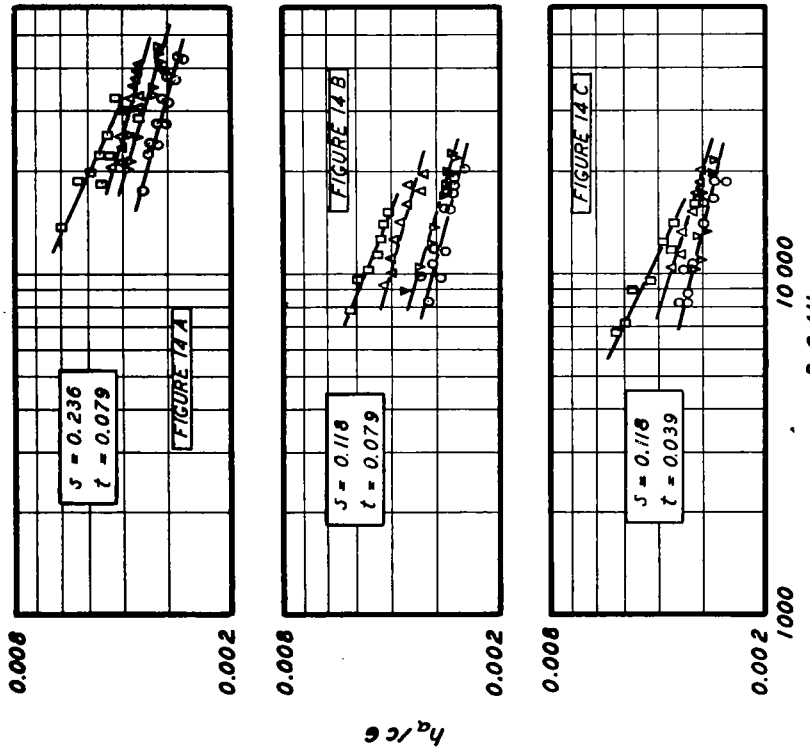

KEY	w	D_b
□	0.275	6.30
△	0.552	6.30
▽	1.101	6.30
○	1.654	6.30

FIGURE 14
STANTON NUMBER VS
REYNOLDS NUMBER FOR
FINNED CYLINDERS SHOWING
THE EFFECT OF FIN WIDTH

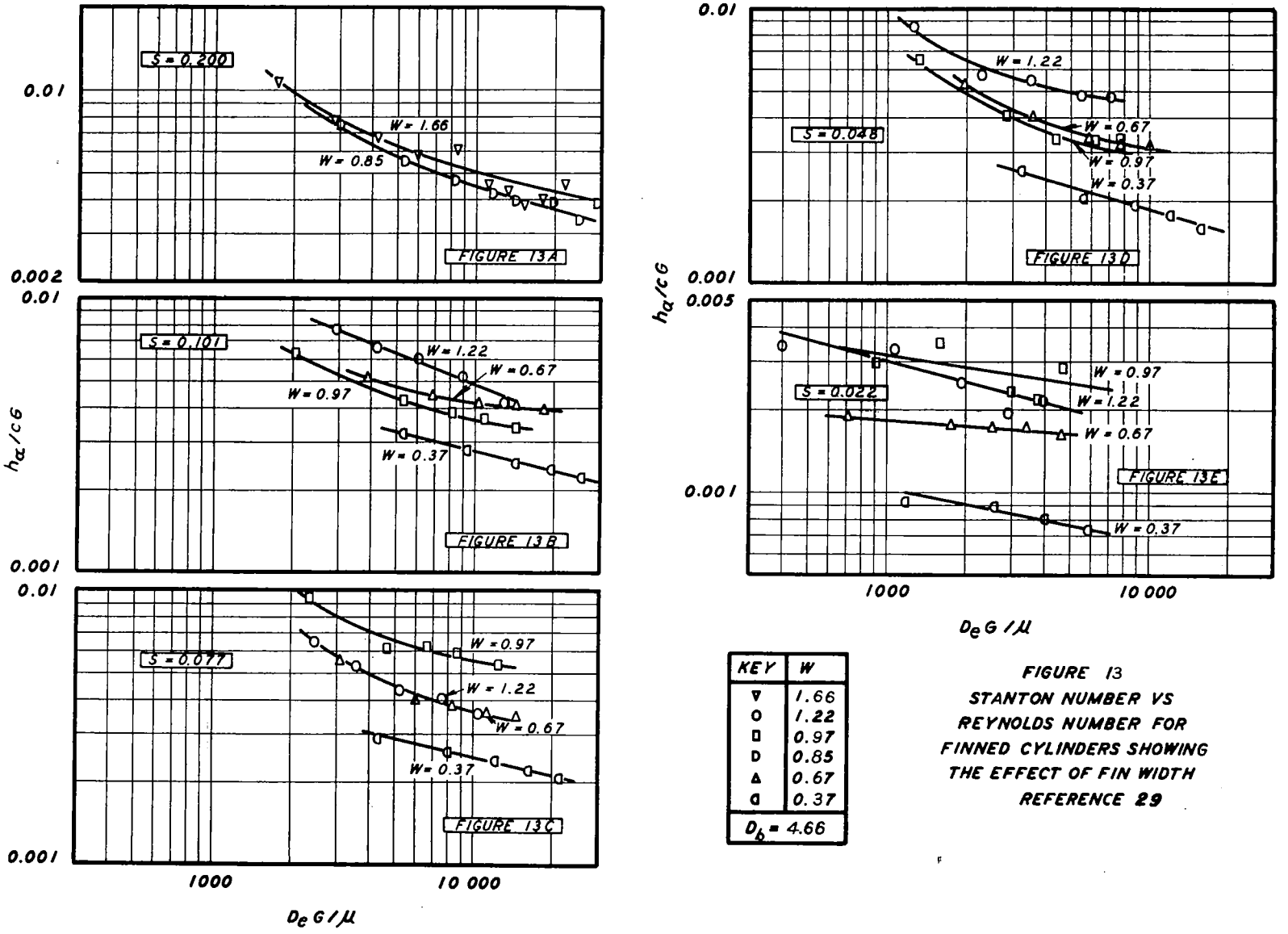

KEY	W
▽	1.66
○	1.22
□	0.97
D	0.85
△	0.67
◁	0.37
D_b = 4.66	

FIGURE 13
STANTON NUMBER VS REYNOLDS NUMBER FOR FINNED CYLINDERS SHOWING THE EFFECT OF FIN WIDTH
REFERENCE 29

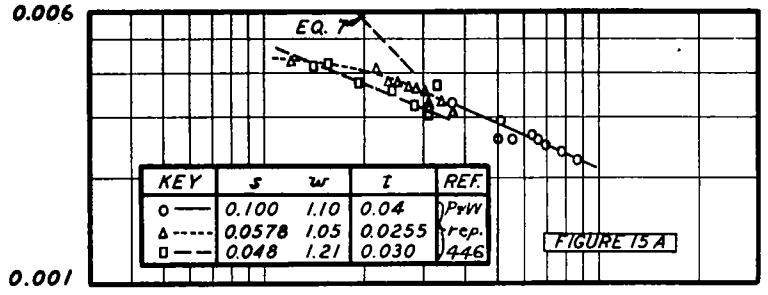

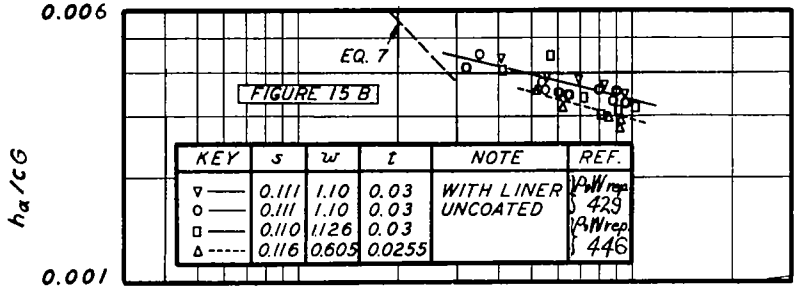

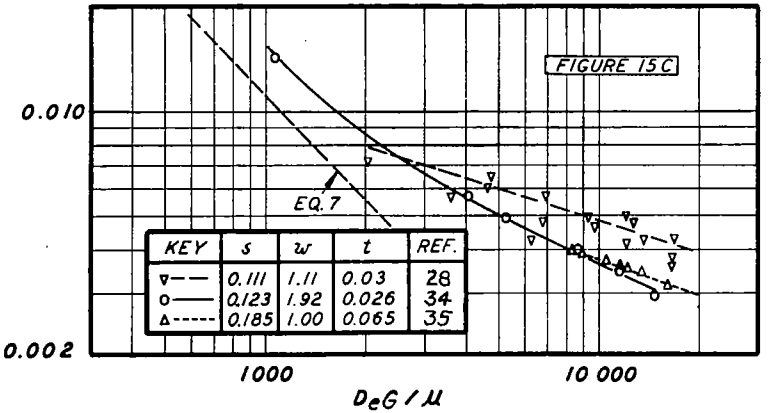

FIGURE 15
STANTON NUMBER VS REYNOLDS NUMBER FOR FINNED CYLINDERS

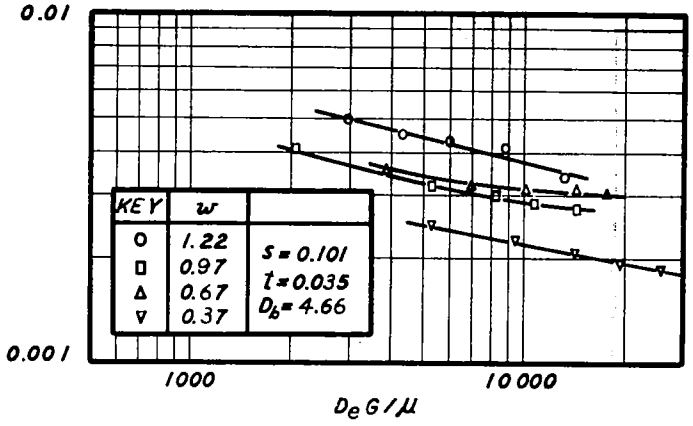

FIGURE 16
STANTON NUMBER BASED ON ΔT_i VS REYNOLDS NUMBER FOR FINNED CYLINDERS SHOWING THE EFFECT OF FIN WIDTH, REFERENCE 29

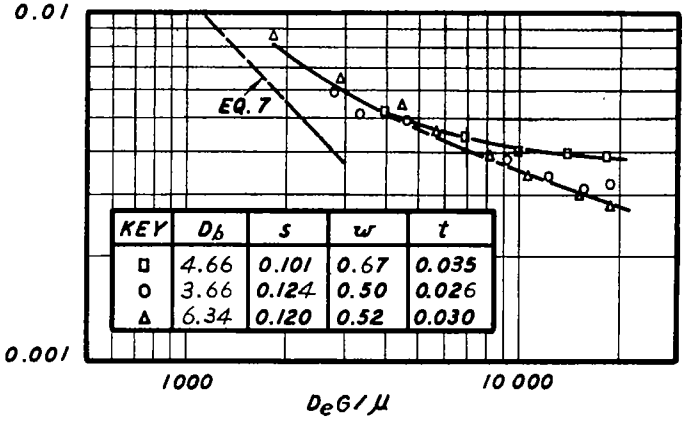

FIGURE 17
STANTON NUMBER VS REYNOLDS NUMBER SHOWING THE EFFECT OF CYLINDER DIAMETER, REFERENCE 29

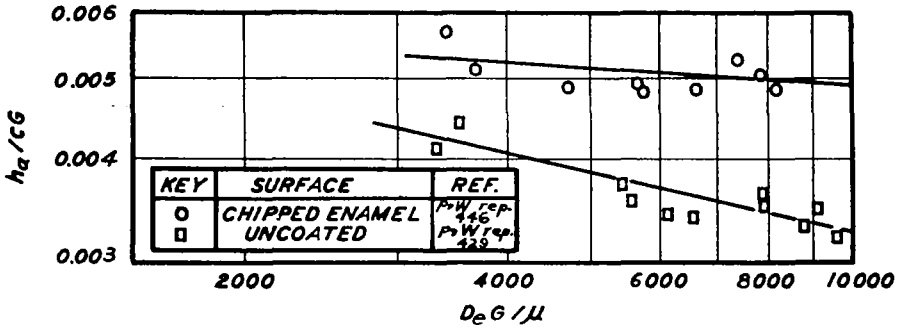

FIGURE 18
EFFECT OF SURFACE ROUGHNESS

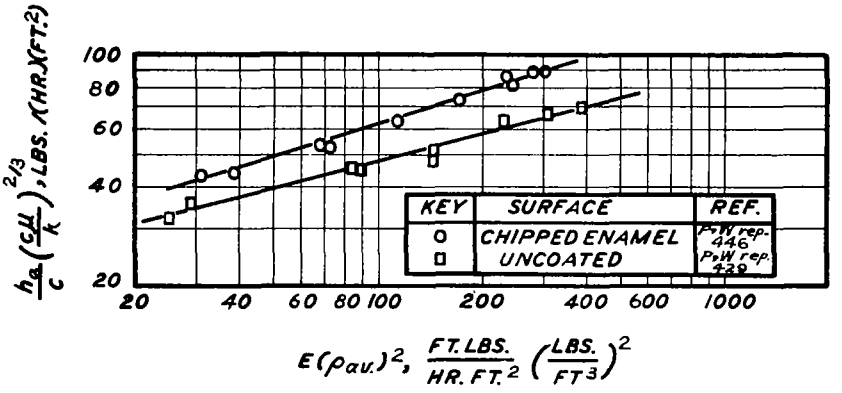

FIGURE 19
EFFECT OF SURFACE ROUGHNESS

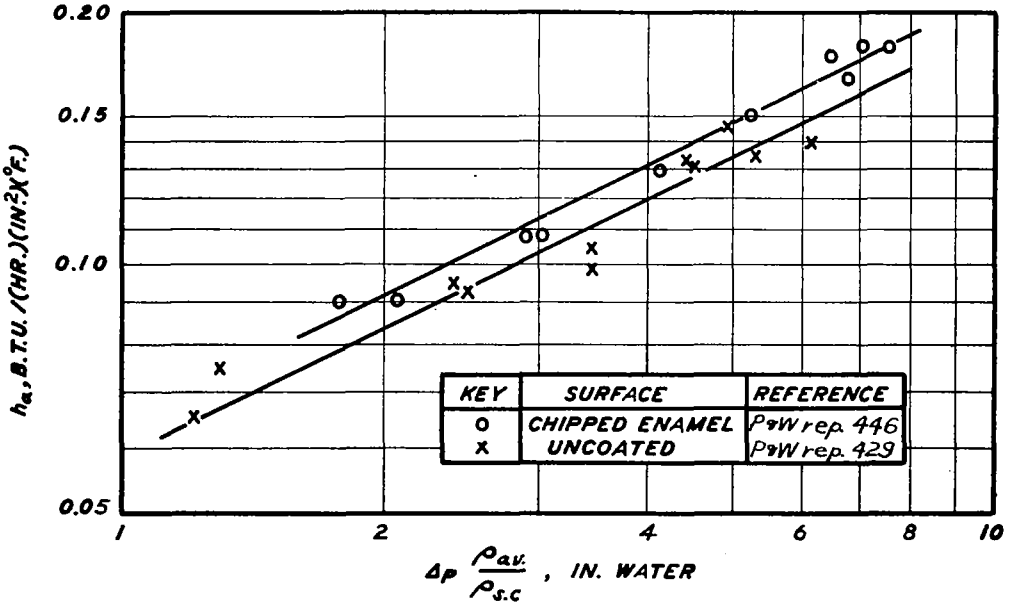

FIGURE 20
EFFECT OF SURFACE ROUGHNESS

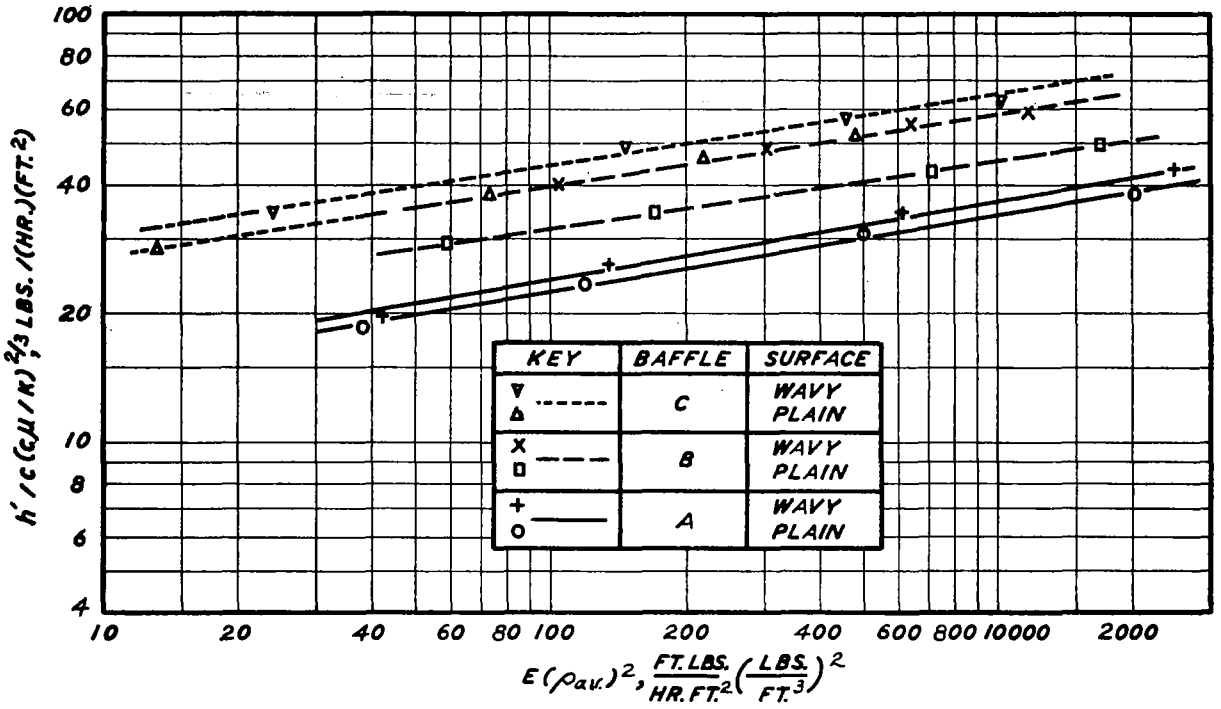

FIGURE 23
EFFECT OF WAVINESS, REF. 37

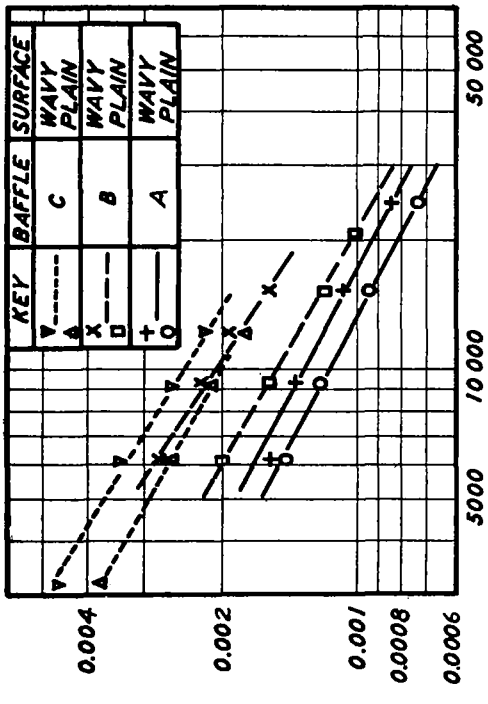

FIGURE 21
EFFECT OF WAVINESS, REF. 37

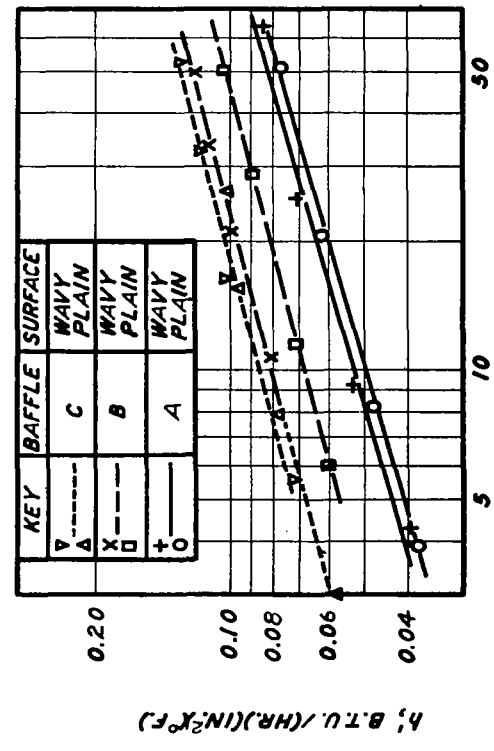

FIGURE 22
EFFECT OF WAVINESS, REF. 37

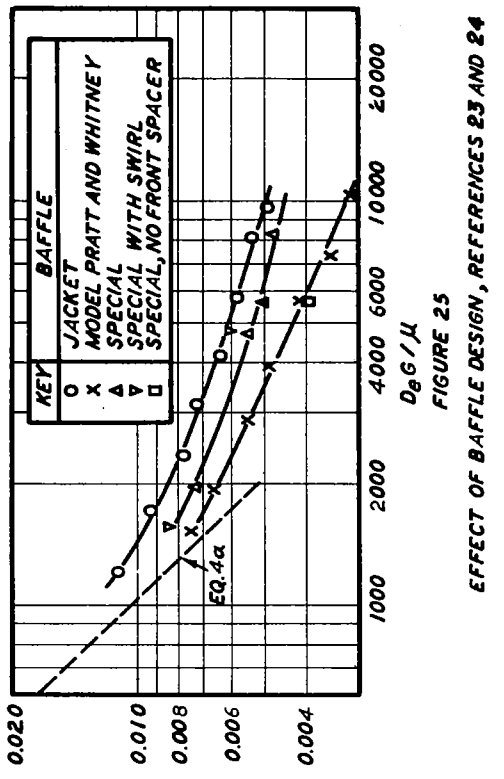

FIGURE 25
EFFECT OF BAFFLE DESIGN, REFERENCES 23 AND 24

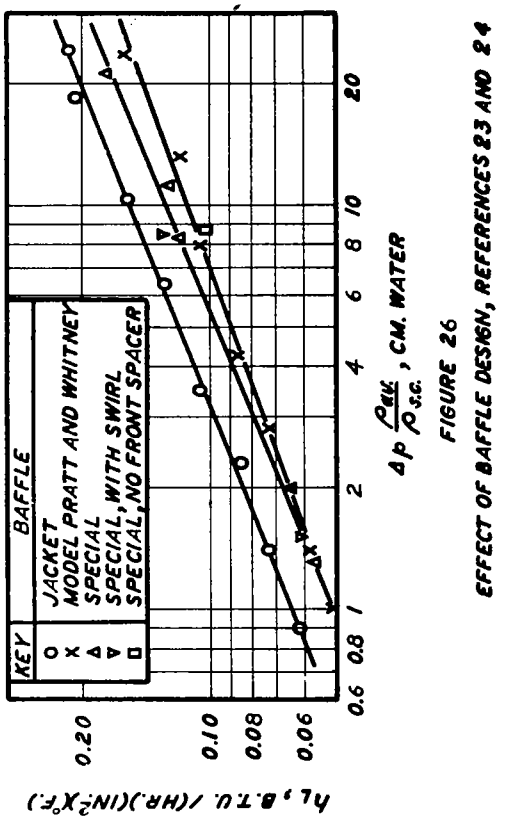

FIGURE 26
EFFECT OF BAFFLE DESIGN, REFERENCES 23 AND 24

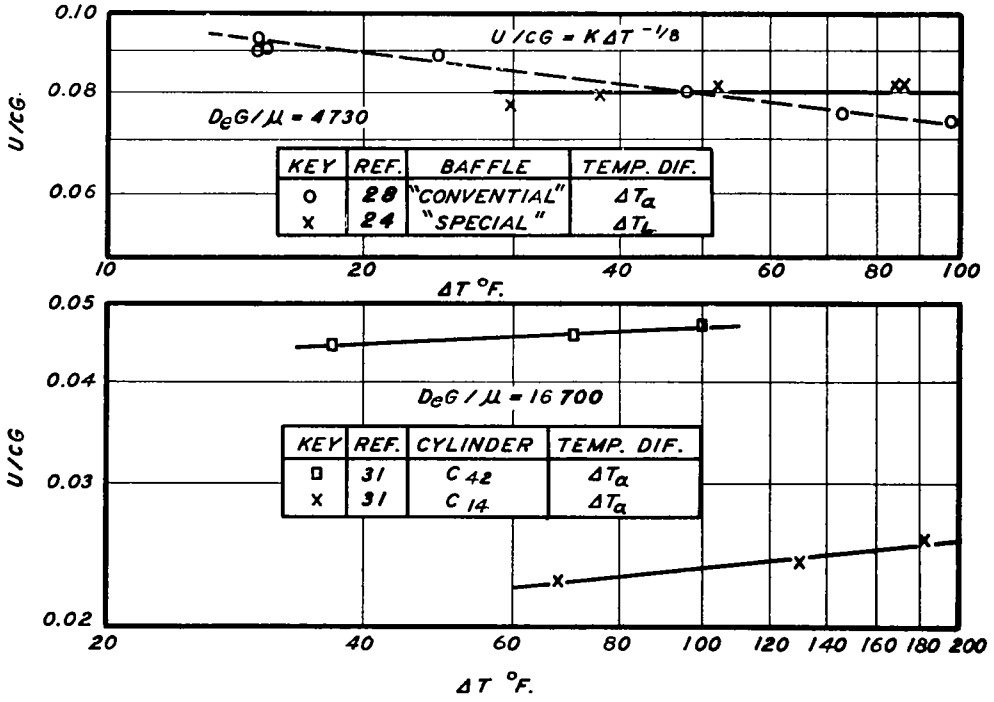

FIGURE 24
EFFECT OF ΔT ON U/cG

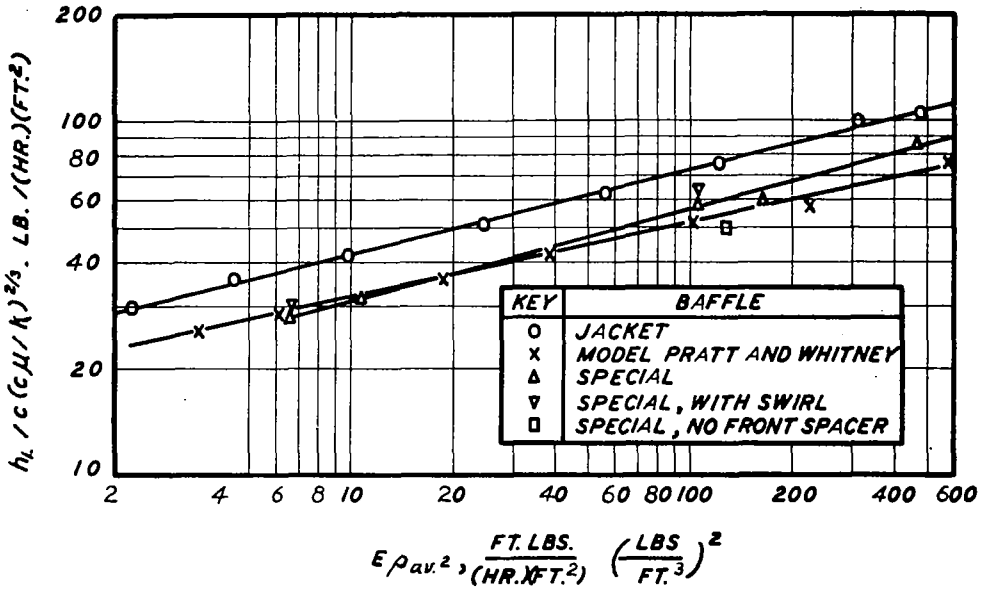

FIGURE 27
EFFECT OF BAFFLE DESIGN, REFERENCES 23 AND 24